Zeitschrift: Eclogae Geologicae Helvetiae
Herausgeber: Schweizerische Geologische Gesellschaft
Band: 86 (1993)
Heft: 1

Artikel: Structural geometry of the Wildhorn Nappe between the Aar massif and the Brienzer See
Autor: Rowan, Mark G.
DOI: https://doi.org/10.5169/seals-167237

Eclogae geol. Helv. 86/1: 87–119 (1993)

0012-9305/93/010087-33 $1.50 + 0.20/0
Birkhäuser Verlag, Basel

Structural geometry of the Wildhorn Nappe between the Aar massif and the Brienzer See

By MARK G. ROWAN [1])

ABSTRACT

The Wildhorn Nappe southeast of the Brienzer See in the Berner Oberland rests directly on sedimentary cover of the Aar massif. The basal detachment is vertical immediately in front of the basement massif and passes through a major synform to horizontal or slight northwest dips. The area is dominated by a Jurassic limestone/marl multilayer which forms kilometer-scale asymmetric buckle folds with moderately-dipping backlimbs and overturned forelimbs.

Although individual folds can be traced for over 30 km along strike (NE–SW), three-dimensional geometries are periclinal rather than cylindrical. Fold hinge lines curve and plunge from central culminations towards both terminations. Hinge line trends for single folds range over 25°, and plunges average 7° to both the northeast and southwest. Axial-perpendicular dilatant veins formed during folding as a necessary consequence of amplification of the periclinal geometries.

Thrust fault ramps underlying the folds are nonexistent, demonstrating that the folds are detachment folds, rather than fault-bend or fault-propagation folds. The few intra-nappe thrusts observed are a response to space problems in overtightened synclines. One, in particular, is interpreted as a late out-of-the-synform thrust caused by re-folding of the entire nappe during thrusting and emplacement of the Aar massif.

Most normal faults in the nappe have small displacements. Whereas some are probably synsedimentary, others are clearly tectonic in origin, and presumably formed due to the orientation of fold limbs in the extensional field of the shear couple defined by the upper and lower nappe boundaries. The two largest normal faults (Sylere and Bürgle faults), however, are anomalous. These have steep southeast dips, maximum displacements of over 1 km, and bound an elongate, overturned limb of the multilayer. They are unlikely to be either synsedimentary, syndeformational, or post-tectonic normal faults. Instead, they may represent early back-thrusts that subsequently rotated during overthrust simple shear.

ZUSAMMENFASSUNG

Die Wildhorndecke südöstlich des Brienzersees im Berner Oberland liegt direkt auf der sedimentären Hülle des Aarmassivs. Der basale Abscherhorizont ist unmittelbar vor dem Aarmassiv vertikal, wird aber in einer Synform gegen Norden zusehends flacher bis horizontal. Das dominierende Element sind die jurassischen Kalk-Mergel-Abfolgen, die in km-grosse asymmetrische Falten gelegt sind. Deren Südschenkel sind mässig steil südfallend, während die Nordschenkel überkippt sind.

Obschon einzelne Falten über 30 km längs des Streichens verfolgt werden können, ist ihre Geometrie eher periklinal als zylindrisch. Die Faltenachsen sind gekrümmt und tauchen von axialen Kulminationen in beiden Richtungen periklinal ab. Für einzelne Falten variieren die Faltenachsen im Azimuth über 25°, und tauchen im Mittel mit 7° nach Nordosten, bzw. Südwesten. Zerrklüfte, senkrecht zu den Faltenachsen orientiert, öffneten sich während der Faltung als direkte Folge der sich verstärkenden Achsenkumulation.

Die Falten sind nicht mit Überschiebungsrampen verknüpft, sind also nicht Rampenfalten (bzw. «fault-bend-» oder «fault-propagation folds»), sondern es handelt sich um Falten, die sich über einem relativ mächtigen Abscherhorizont entwickelten.

[1]) Department of Geological Sciences, University of Colorado, Boulder, CO 80309, USA.

Insbesondere sind die wichtigen Überschiebungen innerhalb dieser isoklinalen Falten als Reaktion auf deren Einengung zu sehen. Eine davon ist als späte Überschiebung anzusehen, die sich im Zusammenhang mit der Aufwölbung des Aarmassivs bildete und dabei eine Synklinale innerhalb der Wildhorn-Decke zerscherte.

Die meisten der Abschiebungen innerhalb der Wildhorn-Decke haben kleine Sprunghöhen. Einige der Abschiebungen mögen synsedimentär gewesen sein, andere sind aber sicher alpintektonischen Ursprungs. Letztere könnten dadurch bedingt sein, dass die Faltenschenkel ins Extensionsfeld zu liegen kamen, welches sich durch die Scherung zwischen Deckenober- und -untergrenze ergab. Die beiden wichtigsten Abschiebungen (die Bürgle- und Sylere Störungen), sind aber anormal. Sie fallen steil nach Südosten ein, besitzen Sprunghöhen von über 1 km und begrenzen einen länglichen Verkehrtschenkel. Sie dürften weder synsedimentären Ursprungs sein, noch während der alpinen Hauptdeformationsphase oder in einer späten Phase angelegt worden sein. Viel eher sind sie in einer frühen Phase als südgerichtete Überschiebung angelegt worden und später durch die einfache Scherung im Zusammenhang mit der Internverformung und Überschiebung der Wildhorn-Decke in ihre heutige Lage hineinrotiert worden.

Introduction

The Helvetic nappes of Switzerland have long played a prime role in the study of nappe tectonics and structure (e.g., Lugeon 1902, Heim 1921). In the areas of the western and eastern Helvetics, especially, detailed investigations have greatly increased the understanding of the geometry, strain, and kinematics of the nappes and their characteristic folds (e.g., Trümpy 1969, Durney & Ramsay 1973, Pfiffner 1978, 1981 b, Ramsay 1981, Dietrich & Casey 1989). Yet the structure and tectonics of the Helvetics of central Switzerland have received relatively little attention, despite their key position between the western and eastern regions.

This paper presents the results of an investigation of a portion of the Wildhorn Nappe in the Helvetic nappes of the Berner Oberland between the Brienzer See and the Aar massif (Fig. 1). This area was initially studied in the early part of this century (Heim 1921, Stauffer 1921, Günzler-Seiffert 1925, 1934a, Günzler-Seiffert & Wyss 1938) and more recently by Pilloud (1990). It was mapped on a reconnaissance level by R. Kligfield during 1978–1980 as part of the ETH (Zürich) team effort, headed by J. G. Ramsay, to provide a regional structural compilation of the Helvetic nappes at a scale of 1:100000. As part of the current project, an area of 300 square kilometers was mapped by the author at a scale of 1:25000, with the emphasis on determining and understanding the three-dimensional fold geometries, kinematics, and strain. A simplified version of the map is shown in Fig. 2, and a more detailed version can be found in Rowan (1991). Although all relevant structural features were examined and analyzed during the course of the study, only the medium- to large-scale folds and faults are presented here. The paper is intended to depict the three-dimensional geometry primarily through the map and the accompanying cross sections.

Stratigraphy

The mapped area is dominated by Jurassic limestones of the Wildhorn Nappe. These form a multilayer bounded below by incompetent Dogger shales at the base of the nappe, and above by lowermost Cretaceous marls. This latter unit essentially serves as an intra-nappe detachment, as the overlying Cretaceous folds are largely disharmonic with respect to those involving Jurassic formations (Ramsay 1981, 1989, Ramsay et al. 1983, Burkhard 1988). The structural disharmony becomes complete farther to the northeast with the formation of two separate nappes (Trümpy 1980).

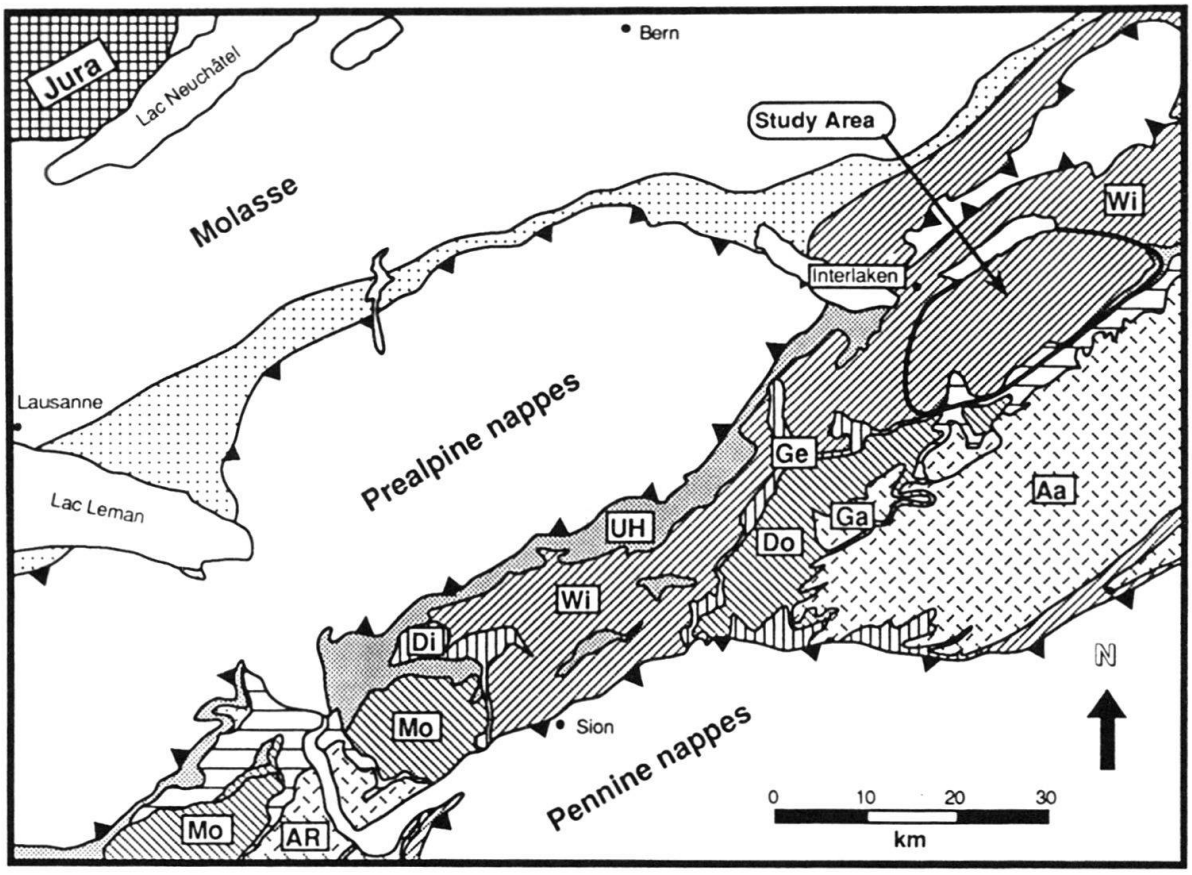

Fig. 1. Tectonic map showing location of study area. Adapted from Masson et al. (1980).

The relevant stratigraphy of the Wildhorn Nappe is shown in Fig. 3 (see also Günzler-Seiffert 1925, Masson et al. 1980, Pilloud 1990). Above the basal detachment, which generally rides on the parautochthonous sedimentary cover of the Aar massif, the following units are found successively higher in the nappe:

1) Glockhaus Formation (Aalenian to Early Bajocian) – dark, micaceous shales with interbedded ferruginous quartzose sandstones. The base is a thicker shale sequence with no sandstones (Basale Tonschiefer). This unit is relatively incompetent, especially towards the base, and has been tectonically thickened in the anticline cores and thinned below the synclines, so that its original thickness is unknown.

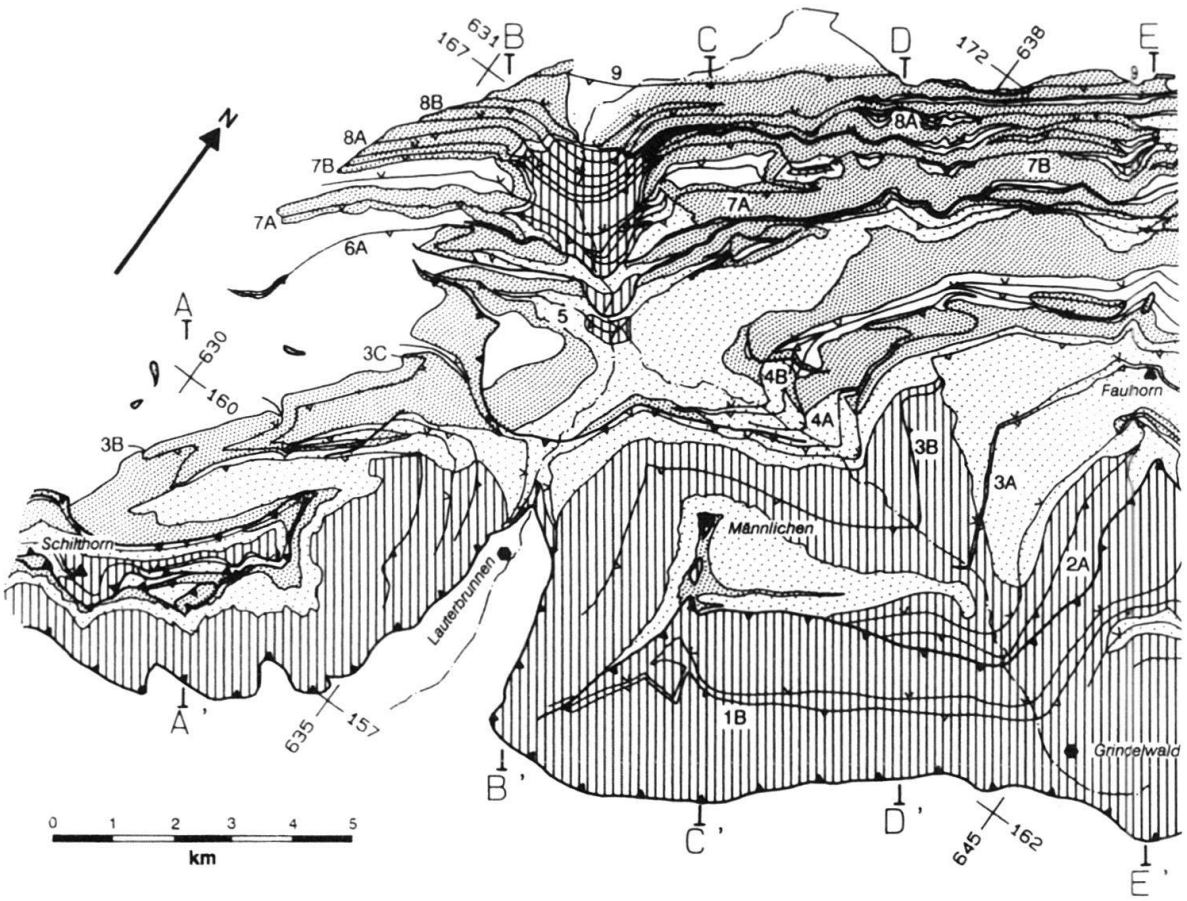

Fig. 2. Structural geologic map of the Wildhorn Nappe, simplified from Rowan (1991), showing location of cross sections A–A′ to G–G′ (Fig. 4). Numbers represent anticline notation which differs from that of Günzler-Seiffert (1934b, 1967) and Pilloud (1982, 1990).

2) Schwarzhorn Beds of the Hochstollen Formation (Bajocian) – interbedded fine-grained clastic marly limestones and marls. The limestones contain echinoderm and other fossiliferous clasts with rare quartz grains, and individual beds range in thickness from 5–60 cm. The intervening marls are between 5–40 cm in thickness. The total thickness of the Schwarzhorn Beds ranges from less than 50 m in the northwest to over 400 m in the southeast, often with significant thinning on fold forelimbs.
3) Echinoderm Member of the Hochstollen Formation (Bajocian) – medium-bedded, medium – to very coarse-grained echinoderm grainstone, dominated by crinoid ossicles and other echinoderm fragments, with micritic pellets and rare quartz grains. The maximum thickness is about 80 m, and the unit pinches out to the northwest.
4) Erzegg Formation (Bathonian to Early Oxfordian) – marls with a total thickness of less than 100 m.
5) Schilt Beds (Middle Oxfordian) – marls with thin interbeds of micritic limestones similar to those of the overlying Quinten Limestone. The thickness ranges up to about 60 m.
6) Quinten Limestone (Late Oxfordian to Tithonian) – medium- to massively-bedded micritic limestone with rare, thin interbeds of marl. This competent, cliff-forming unit

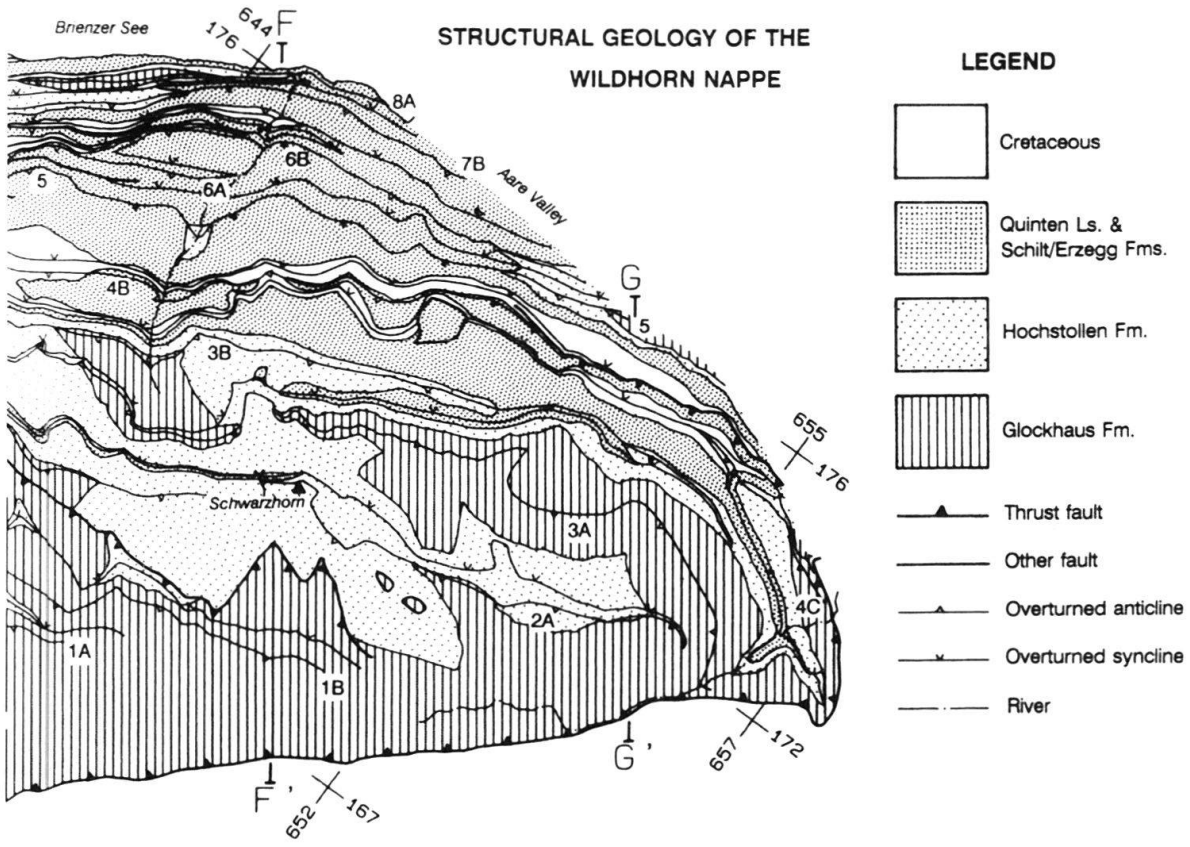

ranges from 150–350 m in thickness, and exerts dominant control on fold wavelengths and geometries.

7) Palfris Shales (Berriasian) – thick, incompetent sequence of marls that divides the Jurassic limestones from those in the Cretaceous, thereby forming the upper boundary to the relatively competent Jurassic multilayer.

All units were mapped separately, with the exception of the Erzegg-Formation and Schilt Beds, which were combined because of their poor exposure and minimal thicknesses. However, for the map reproduced here in Fig. 2, the Schwarzhorn Beds and Echinoderm Member are undifferentiated, as are the Quinten, Schilt, and Erzegg units. The cross sections show the originally mapped formations.

Structure

The Wildhorn Nappe, although it is structurally the highest of the Helvetic nappes, rests directly on the sedimentary cover of the Aar massif throughout the majority of the area mapped. Only in the extreme southwest corner, around the Lauterbrunnen Valley, do the intervening Gellihorn and Doldenhorn Nappes form the immediate footwall (see Masson et al. 1980, Burkhard 1988). The Ultrahelvetic nappes, which are tectonically above the Wildhorn Nappe in other areas, are absent due to erosion.

The basal detachment of the Wildhorn Nappe is approximately vertical along the southeastern margin of the nappe directly in front of the Aar massif, and exposures in

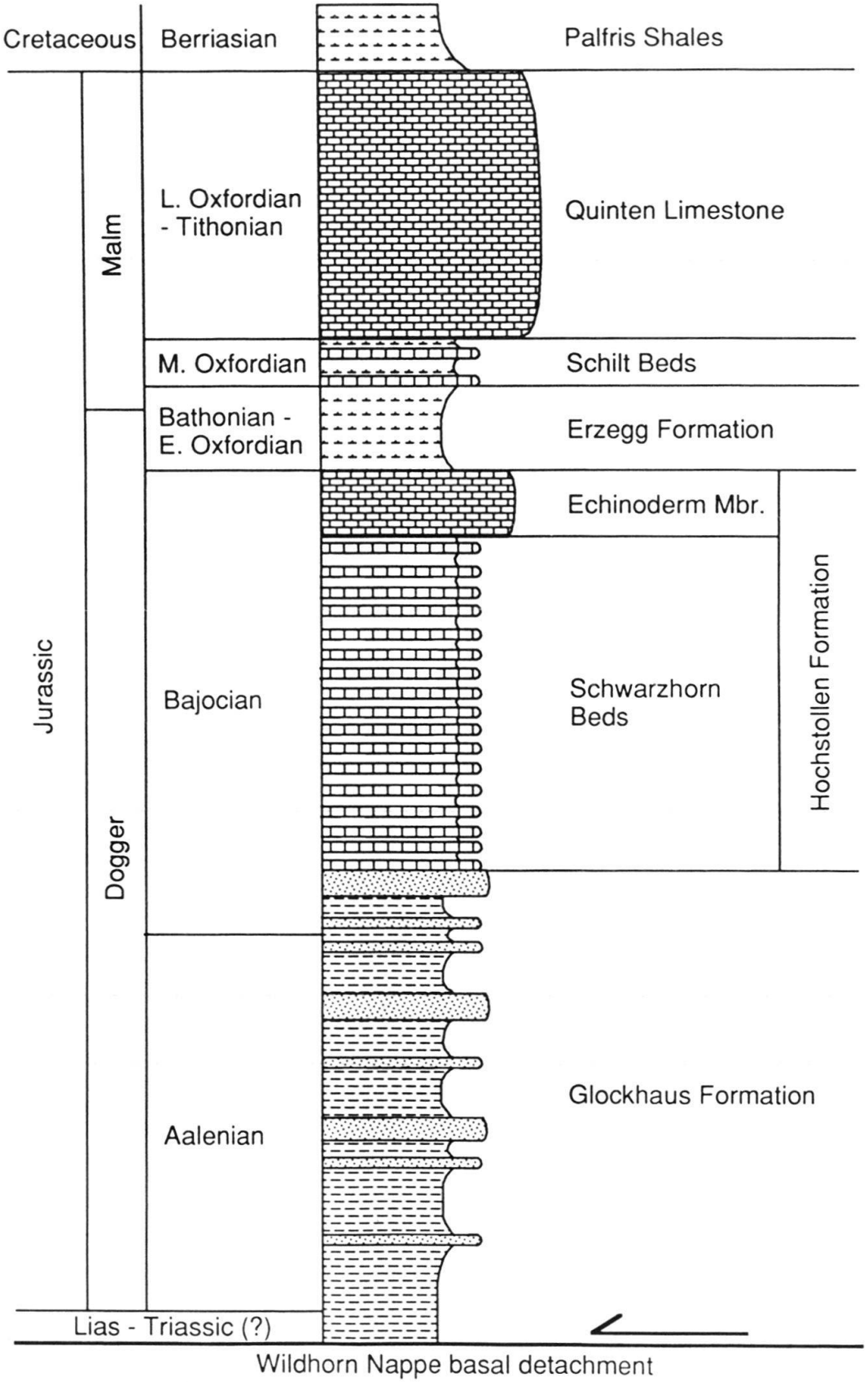

Fig. 3. Stratigraphic column of Jurassic portion of Wildhorn Nappe (not to scale). Width of beds indicates relative competence.

both the Lauterbrunnen and Aare valleys show that it passes through a major synform to slight northwest dips (see Fig. 4). This folding of the entire nappe postdates its emplacement, and was caused by thrusting and uplift of the basement massif (Günzler-Seiffert 1941 b, Burkhard 1988). The basal detachment beneath the rest of the region, however, cannot be observed directly. An approximately level orientation is suggested by the lack of large-scale folding or tilting of the nappe and by mapped Liassic rocks along the shore of the Brienzer See (Pilloud 1990). A similar orientation is suggested by Burkhard (1988, Fig. 10b), who presented a regional contour map of the base of the entire Helvetic nappe complex which places the detachment roughly horizontal at about sea level in the vicinity of the Brienzer See. An exception to the probably horizontal orientation occurs in the southwestern corner of the area, where a regional northwestern tilting of the nappe is related to the presence and emplacement of the underlying Gellihorn and Doldenhorn Nappes.

Folds

Profile geometry

Seven cross sections have been constructed from the field data (Fig. 4). The strike length of the area is 33 km, and the sections are spaced between 3.2 and 5.9 km apart (see Fig. 2 for locations). Bedding, cleavage, and fold axis orientations were used to define subjectively thirty domains of approximately cylindrical folding. For each domain, the mean fold axis was determined statistically; these have a trend range of 57° (039°–096° azimuth) and a plunge range of 19° (10° SW–9° NE). Data in each domain were projected along the domain axes into vertical sections, which are the best approximations to true cross sections because the regional mean fold axis is horizontal, with only local southwest or northeast plunges. Orientation data and contacts within 1 km of each section were generally projected, although some points were projected up to a maximum of 2.5 km.

The cross sections are simplified in that small-scale parasitic folds, small-scale normal and reverse faults, and localized warping of bedding are not shown. In addition, there are regions where the geometries are poorly constrained, and the relative certainty of the depicted geometries is indicated in Fig. 4 by the line type. The dotted pattern denotes speculative projection into: firstly, areas in which the upper (Malm) levels have been eroded; secondly, areas of relatively poor outcrop (e.g., the forested slope above the Brienzer See); and thirdly, deep levels away from the large Aare and Lütschine valleys. It is stressed that, in these regions, the sections have been constructed using the appropriate structural styles than can be observed directly in adjacent areas. Thus, for example, the eroded Quinten Limestone in the southeastern portions of the sections is shown to be folded harmonically with the underlying Dogger formations, because this is the relationship that is generally observed where the Quinten Limestone is preserved. Complicated geometries, such as those found in the Oltschiburg and Schilthorn areas, are anomalous (see below) and have not been introduced. Comparison of the interpretations shown in Fig. 4 with the sections of Stauffer (1921), Günzler-Seiffert (1943 b, 1967), and Pilloud (1990) is discussed later, although it is noted here that a fold notation system (numbered labels in Figs. 2, 4, 5, 8), different from that defined by Günzler-Seiffert and

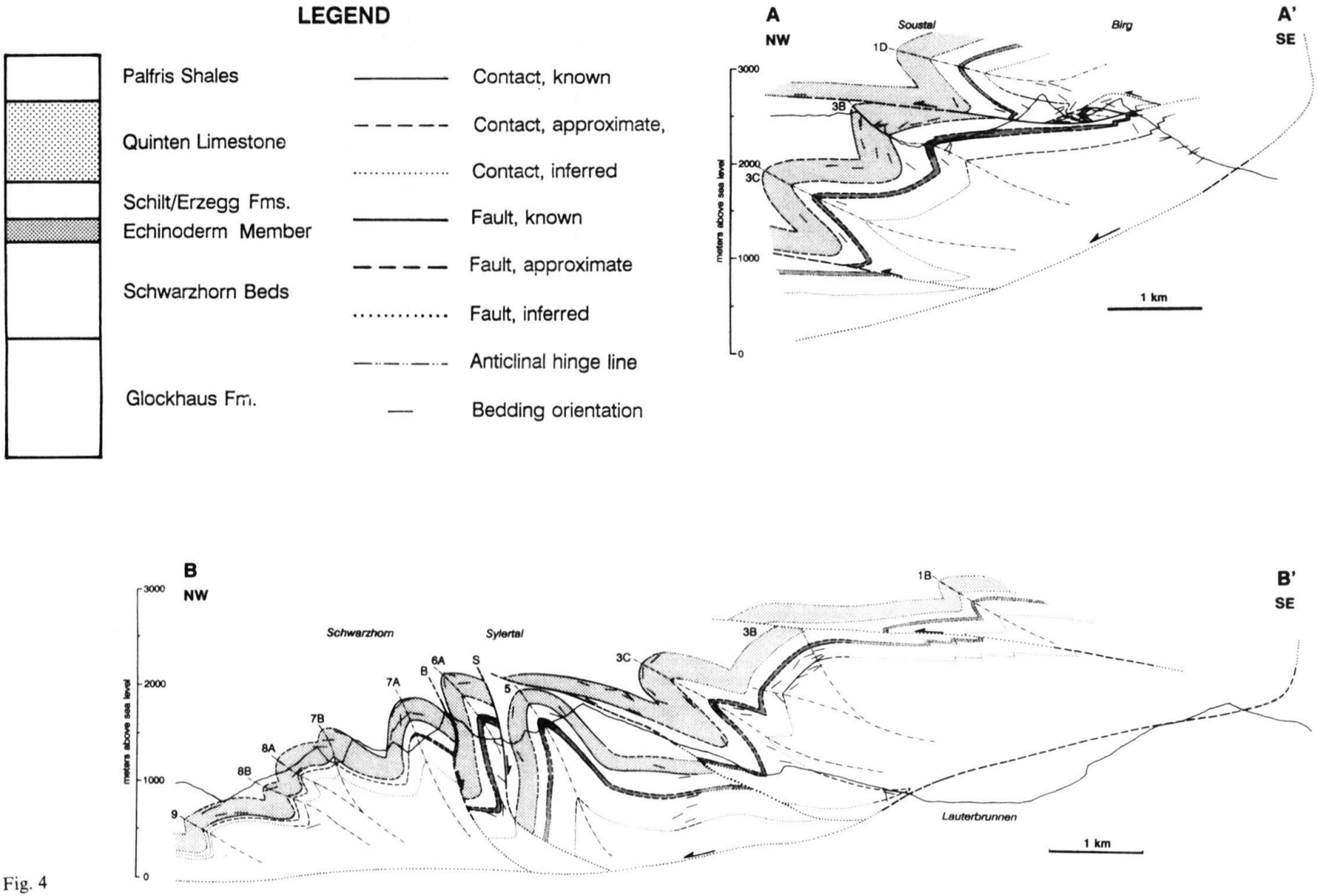
LEGEND
Palfris Shales
Quinten Limestone
Schilt/Erzegg Fms.
Echinoderm Member
Schwarzhorn Beds
Glockhaus Fm.
Contact, known
Contact, approximate,
Contact, inferred
Fault, known
Fault, approximate
Fault, inferred
Anticlinal hinge line
Bedding orientation
A
NW
Soustal
Birg
A'
SE
1D
3B
3C
3000
2000
1000
0
meters above sea level
1 km
B
NW
Schwarzhorn
Sylertal
B'
SE
1B
3B
3C
6A
B
S
7A
5
7B
8A
8B
9
Lauterbrunnen
1 km

Fig. 4

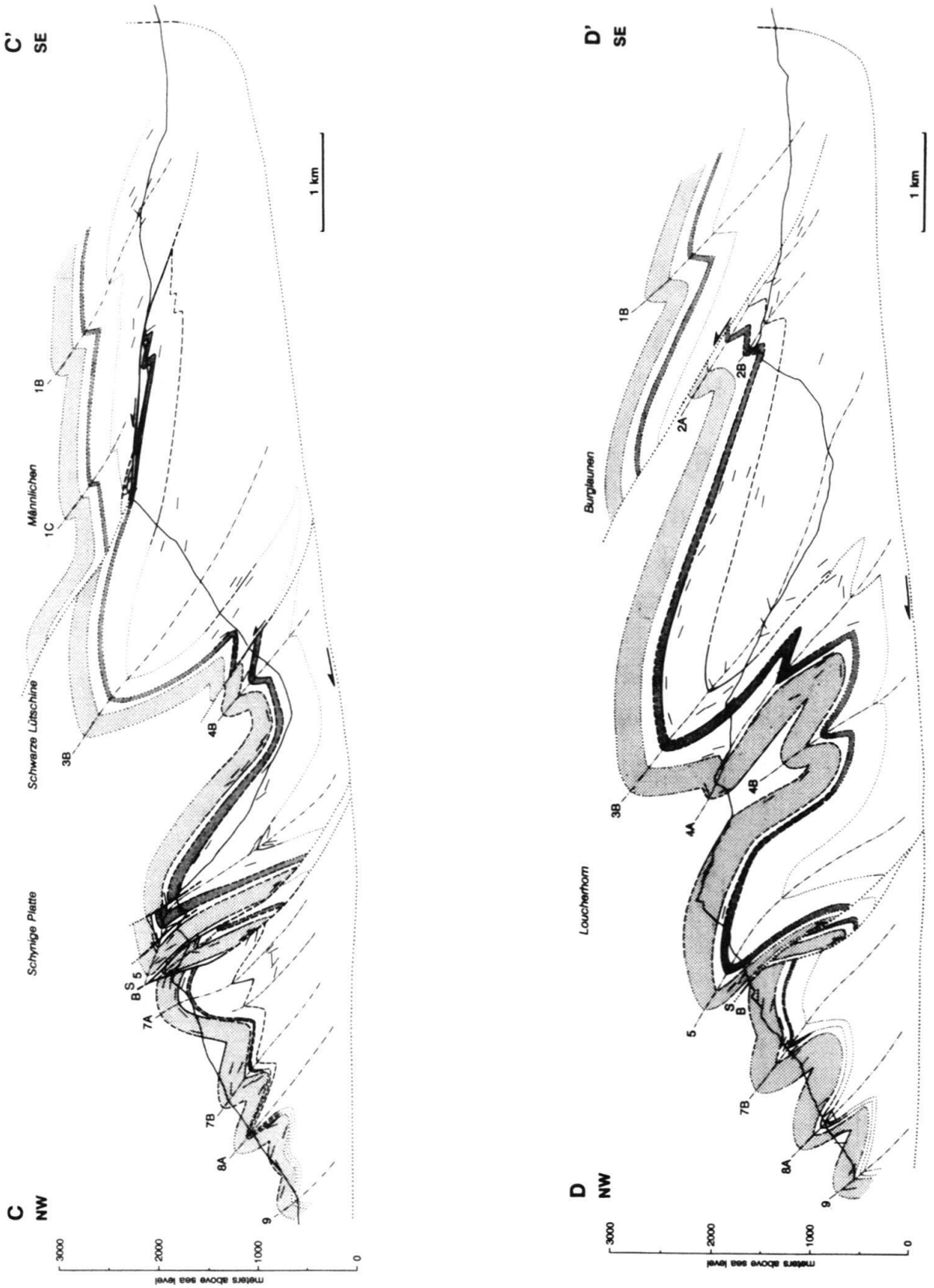
C'
SE
C
NW
Männlichen
Schwarze Lütschine
Schynige Platte
1B
1C
3B
4B
5
7A
7B
8A
9
1 km
3000
2000
1000
0
metres above sea level
D'
SE
D
NW
Burglauenen
Loucherhorn
1B
2A
2B
3B
4A
4B
5
7B
8A
9
1 km
3000
2000
1000
0
metres above sea level

Fig. 4

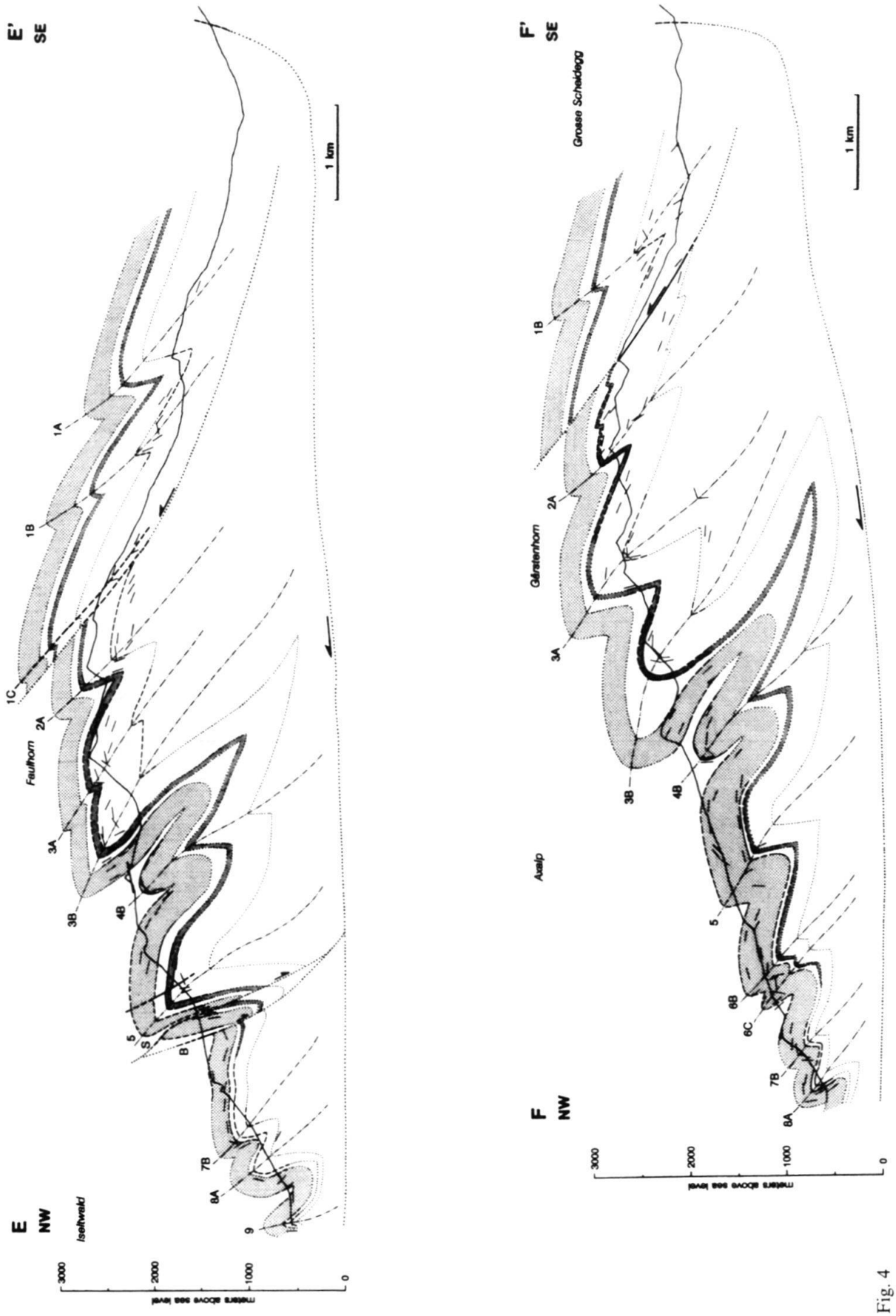
E
NW
Iselwald
E'
SE
Faulhorn
1 km
F
NW
Aaalp
F'
SE
Grosse Scheidegg
Gätstenhorn
1 km
3000
2000
1000
0
Meters above sea level

Fig. 4

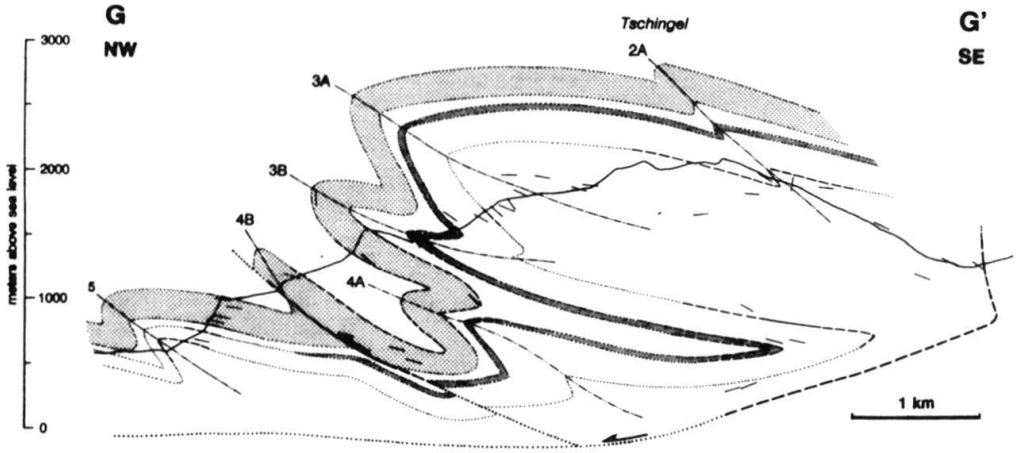

Fig. 4. NW–SE structural cross sections through field area (locations shown in Fig. 2). Anticline notation corresponds to that in the text and Figs. 2 and 8, but not to that of Günzler-Seiffert (1934b, 1967) and Pilloud (1982, 1990).

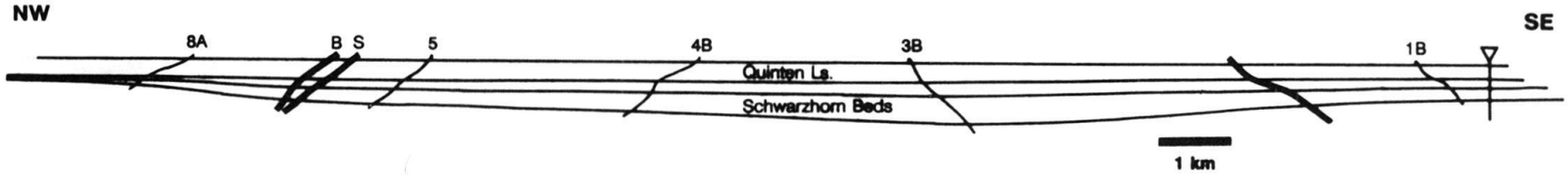

Fig. 5. Key-bed and area restoration (using the software GEOSEC-20) of section D–D′ from Fig. 4, indicating a net shortening during folding of 48%. Bed lengths at the top and bottom of the Quinten Limestone, the Echinoderm Member, and the Schwarzhorn Beds are equal to those in the deformed section, and the area of each unit is maintained. The Glockhaus Formation is not restored because of lack of constraints. The pin-line, located on the backlimb of fold 1 B, is constrained by kinematic criteria (Rowan 1991). Thin lines with numbers are the undeformed trajectories of fold axial traces, thick lines are those of faults. **S** and **B** are the Sylere and Bürgle faults, respectively; note that these had original northwest dips.

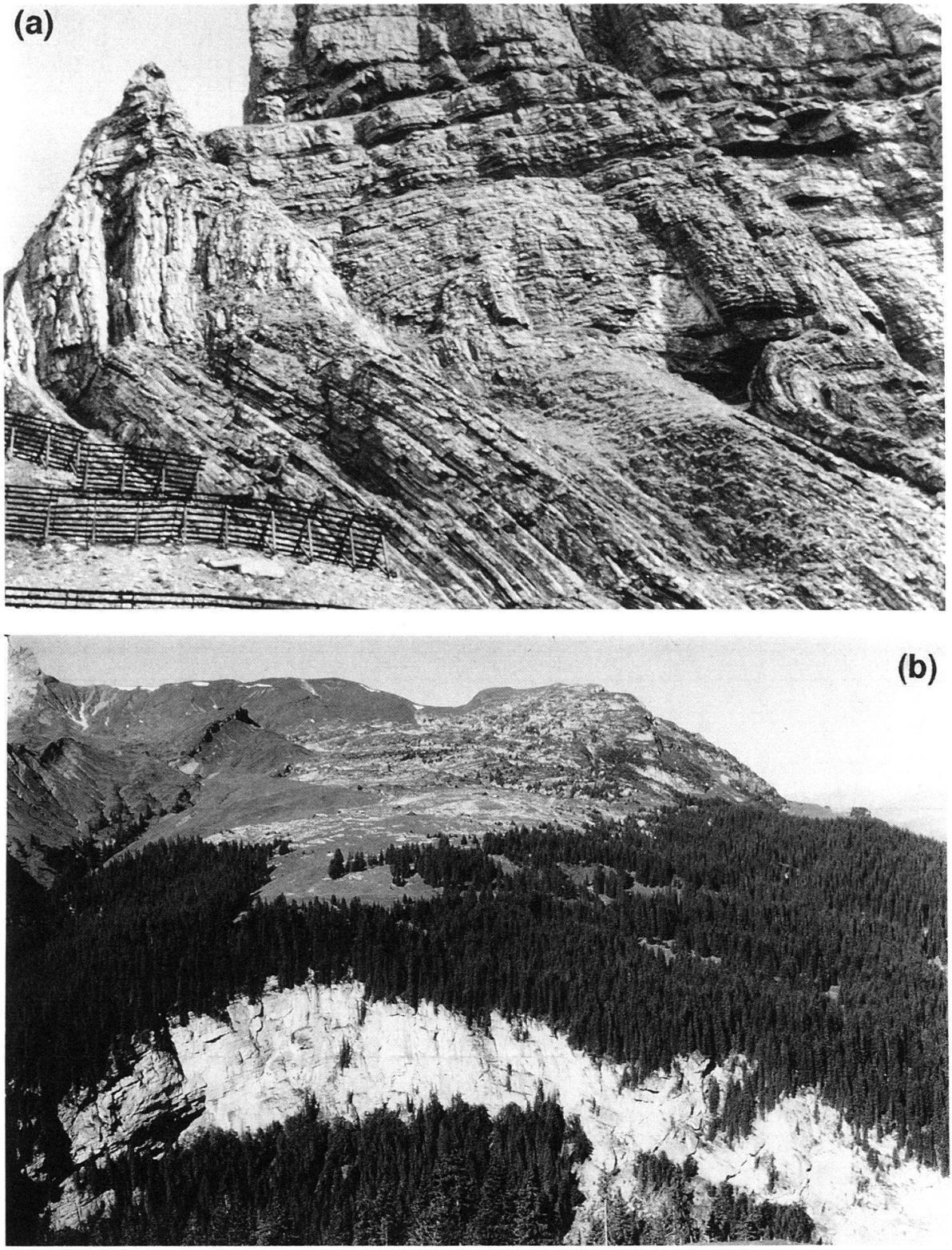

Fig. 6. a) Hinge of fold 3 B in Schwarzhorn Beds. View towards NE at grid reference 639.75, 167.4. Note angular geometry and thinning of beds in overturned limb. Height of avalanche fences is approximately 3 m. b) Rounded crestal portion of fold 5 in Quinten Limestone. View towards SW at grid reference 644.7, 172.8. Fold is plunging toward viewer from Litschgiburg in background. Height of cliff is approximately 150 m. c) Recumbent, isoclinal syncline in Schwarzhorn Beds, with selected beds outlined. View towards E at grid reference 635.65, 162.4 (north of Lauterbrunnen). Upper, overturned limb is lighter color because of thinning of dark marls. Height of cliff is approximately 180 m. d) Small-scale parasitic fold in Schwarzhorn Beds, with thinning of both limestones and marls in overturned limb. Vertical dimension of photograph is approximately 15 m.

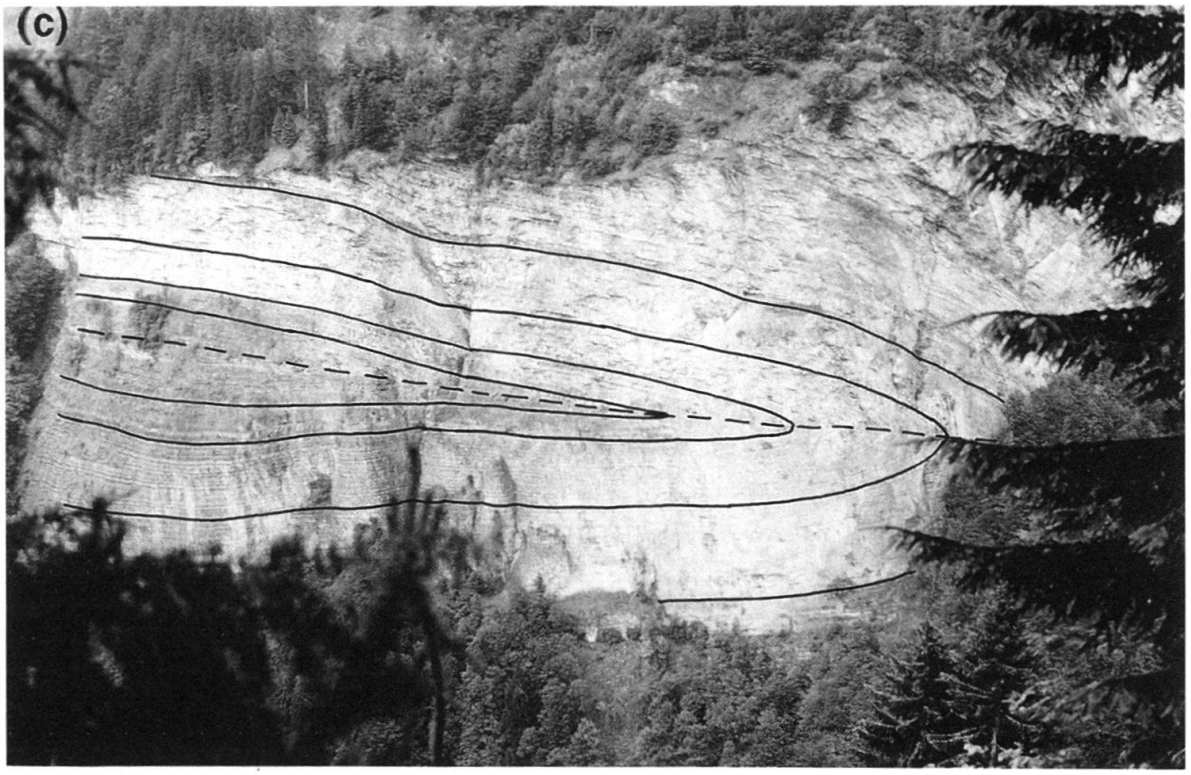
(c)

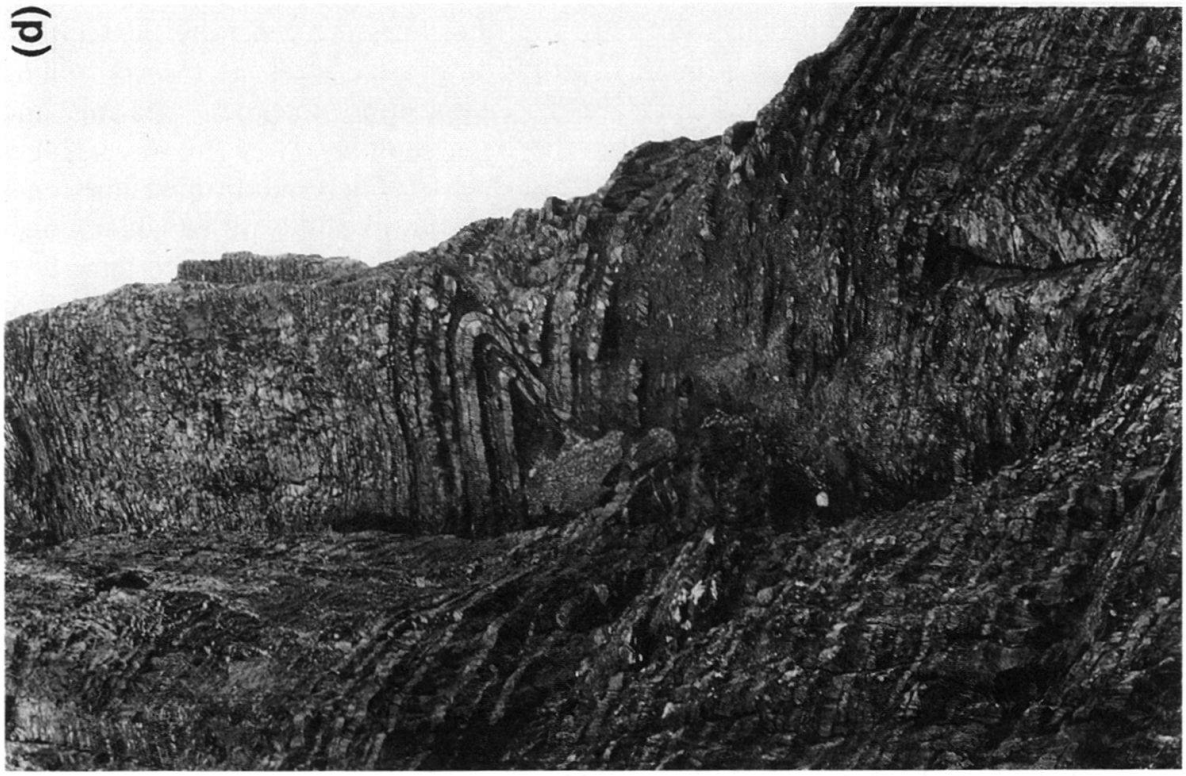
(d)

used by all subsequent workers, has purposely been adopted because of incompatibility of the old system with the current interpretation.

All sections have been constructed so that bed lengths of competent units are roughly equal, as shown in the key-bed and area restoration of section D–D′ (Fig. 5). Bed lengths between the top of the Quinten Limestone and the top of the Glockhaus Formation vary by no more than 10% of the restored section length; differences may be caused by small- to medium-scale deformation (e.g., parasitic folds, small faults, solution cleavage, dilatant veins) or by improper projection of the fold geometries. Restoration of the other sections shows similar undeformed geometries and consistent net shortening of between 45–50%. The restoration is pinned on the backlimb of fold 1 B because of evidence that backlimbs have undergone little layer-parallel shear (Rowan & Kligfield 1992). The divergence between the restored axial planes of folds 3 B and 5 is consistently found on lines B–B′ to E–E′. These are the same lines where the Sylere and Bürgle faults are found, and fold formation may have been influenced by preexisting offsets along these structures (see below).

The Wildhorn Nappe comprises asymmetric detachment folds with maximum amplitudes of 2300 m and maximum wavelengths of 2500 m between the major anticlines. The folds are generally characterized by backlimbs with gentle southeast dips, crestal domains with low northwest dips, and forelimbs with steep northwest to overturned southeast dips. Although folds typically have straight to slightly curved limbs with interlimb angles of 30–60° (Fig. 6a), a wide spectrum of shapes is found, from open, rounded folds (Fig. 6b) to recumbent, isoclinal folds (Fig. 6c). Synclines are generally tighter than anticlines, but geometries vary primarily with stratigraphic level, as the controlling factors in determining the fold shapes are the composition, thickness, spacing, and competence contrasts of the different beds in the folded multilayer (see Ramsay & Huber 1987, p. 405–424). Thus, the Schwarzhorn Beds, which are finely interbedded limestones and marls without major incompetent units, form chevron-like folds with angular hinges (Fig. 6a). The Quinten Limestone, on the other hand, is a thick, massive limestone bounded above by a thick sequence of incompetent shales, and forms folds with rounded hinges (Fig. 6b) and cuspate-lobate geometries typical of strong competence contrasts (see Ramsay 1982).

The fold geometries show significant variations from northwest to southeast. The internal (southeastern) portion of the area is dominated by two large-amplitude and large-wavelength anticlines (folds 3 B and 5), whereas the frontal segment is characterized by a fold train with smaller amplitudes and wavelengths. The change is coincident with a pronounced reduction in the original thickness of the Hochstollen Formation (Figs. 4, 5), providing further evidence that fold shapes are dictated by the thickness and nature of the competent layers in the folded multilayer. This can be seen clearly in Fig. 7: as the thickness of the multilayer increases, the arc length, and thus fold amplitude and wavelength, also increases. Although this relationship is predicted in a general sense by classic buckling theory (e.g., Ramberg 1970a, b), no further attempt has been made to apply the relatively simple mathematical models because of their inability to represent adequately the complicated combination of bed thicknesses and competencies found in the real multilayer of the Wildhorn Nappe.

In addition to original stratigraphic thickness variations, there are thickness changes which are tectonically controlled. First, incompetent units tend to thicken in fold hinges

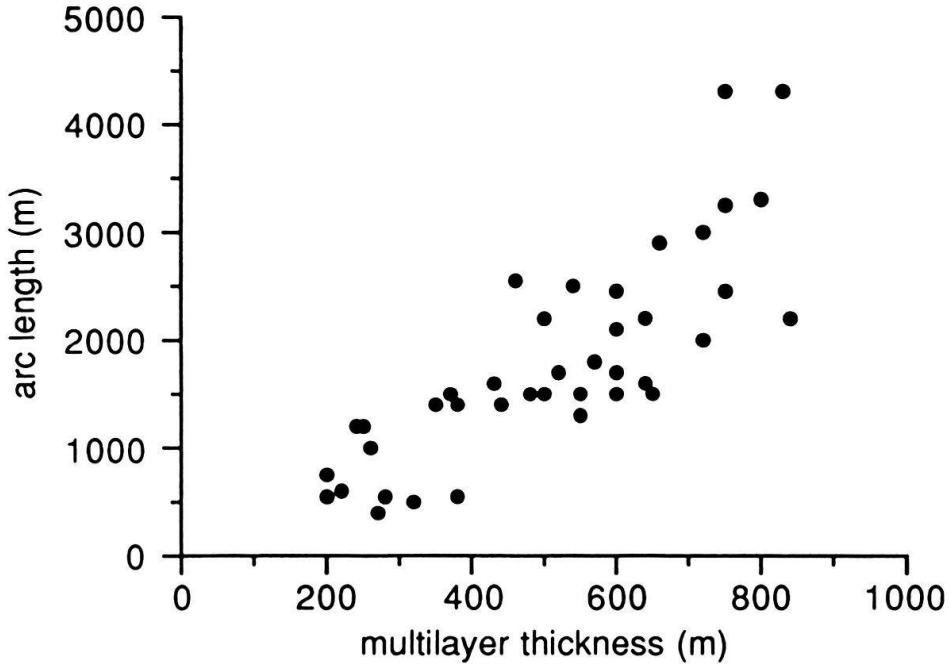

Fig. 7. Plot of fold arc length (measured between anticlinal hinges) versus multilayer thickness (top Quinten Limestone to base Schwarzhorn Beds), showing a general positive correlation as predicted by buckling theory.

and thin on fold limbs. In the case of the Erzegg and Schilt Formations, hinge thickening often accommodates different hinge geometries in the adjacent Echinoderm Member and Quinten Limestone (e.g., fold 3B, section F–F'). Note, however, that folding is still harmonic. In the case of Glockhaus Formation, significant thickening in anticline cores and thinning below synclines accommodates potential space problems caused by the formation of detachment folds. Second, overturned limbs are often structurally thinned. This is especially true for the Schwarzhorn Beds, which show a pronounced forelimb thinning (Fig. 6a, c, d) produced by net volume loss along solution cleavage in both the marls and interbedded limestones (Rowan et al. 1991). The more competent Quinten Limestone and Echinoderm Member typically are not thinned on forelimbs. This is possibly due to the low clay contents of these rocks, which may inhibit the movement of dissolved ions into the free-fluid system for large-scale advective mass transfer (Marshak & Engelder 1985, Rowan et al. 1991). An exception is found in the faulted zone immediately northwest of fold 5, where both units are sometimes thinned significantly. In this case, removal of large amounts of rock volume is probably unrelated to the original clay content and may have been facilitated instead by pervasive fracturing.

Small-scale parasitic folds (Fig. 6d) are common features throughout the area. They are found in all lithologies on both limbs, and more rarely in fold hinges. The shapes mimic those of the large-scale folds, in that parasitic folds in the Schwarzhorn Beds have chevron geometries with angular hinges and substantial forelimb thinning (Fig. 6d), whereas those in the Quinten Limestone have more rounded hinges and minimal thinning.

The folds contain numerous small-scale deformation structures. A spaced solution cleavage is well developed, especially in beds with high clay content, and displays classic cleavage refraction patterns (convergent and divergent fans). However, there is a differ-

ence in pattern between the backlimbs and forelimbs, in that the cleavage is at a much smaller angle to bedding in incompetent beds of the forelimbs, a result of enhanced bedding-parallel slip in this domain during deformation (Rowan 1991, Rowan & Kligfield 1992).

Other small-scale deformaton features include multiple sets of calcite-filled dilatant veins as well as calcite fibers formed along bedding planes during flexural-slip folding. The veins occasionally form en-echelon arrays that accommodate small amounts of simple shear deformation, but more often are isolated tabular veins that formed in response to the imposed far-field and local stress regimes. Although they are generally filled with blocky, rather than fibrous, calcite, they often divide and pass laterally into discrete microscopic crack-seal veins at their terminations, indicating that they grew in episodes of incremental opening. Where fibers are present, they are usually perpendicular to the vein boundaries, so that the veins originated as tensile, rather than shear, fractures.

The veins, cleavage, and other structures are useful indicators of the kinematic development of the folds. Measurement and analysis of the orientations and relative timing of these features in the various structural domains (e.g., forelimbs) suggests that the folds formed as buckle folds in overthrust shear between nappe boundaries at a low angle to originally horizontal bedding (Rowan & Kligfield 1992 and references therein). Furthermore, it has been shown that the folds initiated as symmetric buckles, with little early layer-parallel shortening, and developed their asymmetry by subsequent rotation of fold limbs and axial planes during the northwest-directed simple shear. Quantification of the strain partitioning and forward modelling of the progressive deformation indicates that the dominant process was flexural slip/flow, with added components of brittle fracturing, chemical dissolution, and possibly tangential longitudinal strain (Rowan 1991).

Three-dimensional geometry

The Helvetic nappes are known for their lateral continuity in structural style (e.g., Günzler-Seiffert 1941 a, b, Pfiffner 1978, Ramsay 1981). Ramsay (1989) has shown that individual folds in the Wildhorn Nappe of the western Helvetics can be traced laterally for over 35 km with little change in hinge line trend, and remarked that correlatable folds continue for many tens of kilometers to the northeast into the central Helvetics. Because of this lateral persistence, the Helvetic folds are often considered to be good examples of cylindrical folding, and cylindrical projection techniques have been used to construct profile sections from data spanning a strike distance of well over 5 km (e.g., Ramsay 1981, Langenberg et al. 1987, Dietrich & Casey 1989). Other authors, however, have noted the less-than-cylindrical nature of Helvetic nappe folds (e.g., Pfiffner 1978).

Individual folds within the study area are also laterally persistent, several continuing along the entire 30 km strike length of the mapped region (Fig. 8). However, the fold shapes generally change noticeably over this distance. For example, as fold 5 is followed from southwest to northeast, it loses amplitude, the crestal region widens, and the backlimb becomes more gently dipping. Fold 3 B, from a culmination in the center of the

Fig. 8. Block diagram created from serial sections of Fig. 4. Three-dimensional geometry is shown at the top of the Echinoderm Member. Anticline labels correspond to those in Figs. 2, 4, 5 and text.

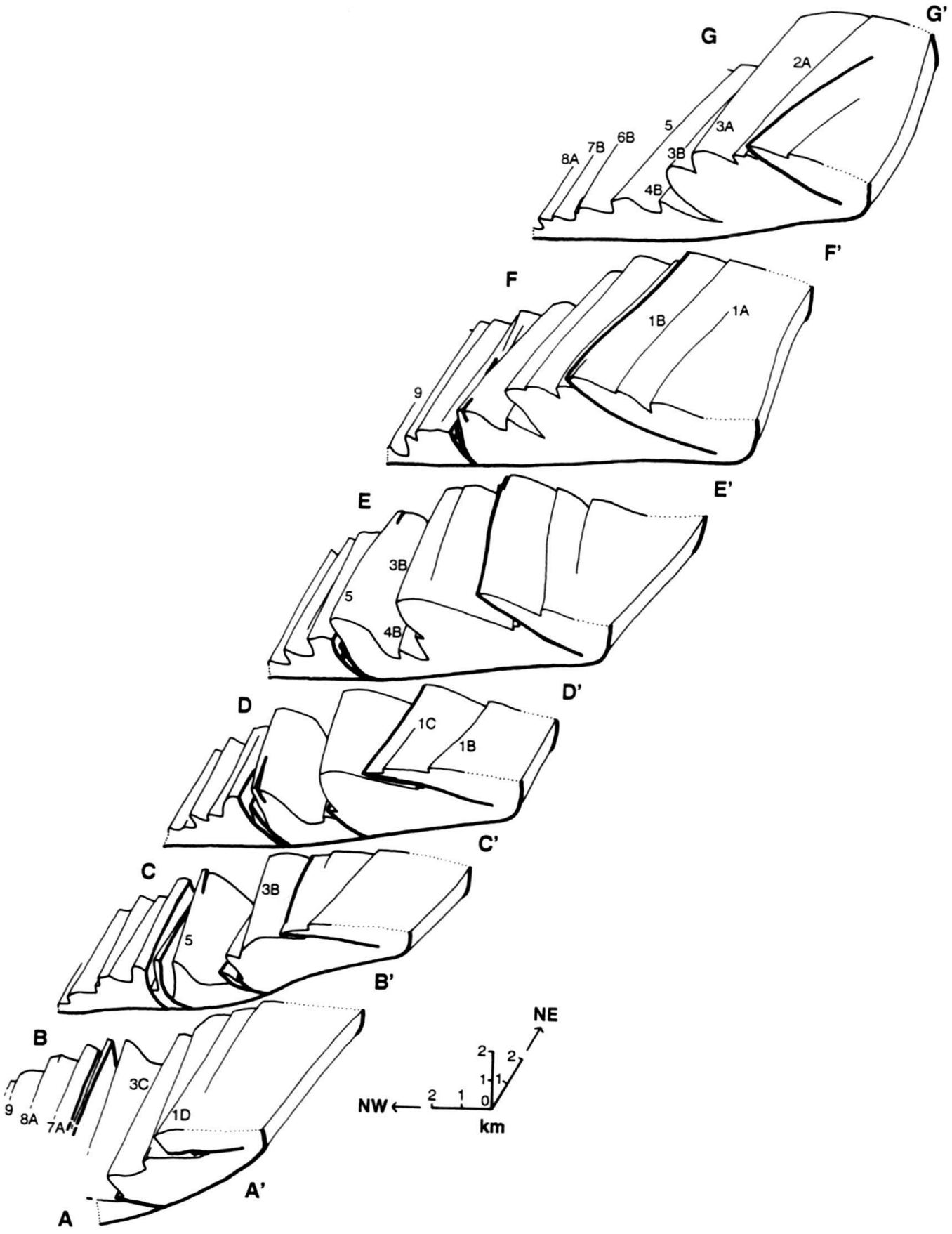
G
G'
2A
5
3A
8A
7B
6B
3B
4B
F
F'
1B
1A
9
E
E'
3B
5
4B
D
D'
1C
1B
C
C'
3B
5
B
B'
3C
9
8A
7A
1D
A
A'
NE
NW
2
1
0
km

area (section D-D'), plunges to the northeast and dies out just before the Aare Valley, and, in plunging the opposite direction to the southwest, changes shape to a more rounded, doubly-hinged fold (section B–B'). In addition, the shortening accommodated by fold 3 B is relayed to adjacent en-echelon folds in both directions: fold 3 A quickly grows on the backlimb of fold 3 B as 3 B dies out to the northeast, and fold 3 C does the same on the forelimb of fold 3 B to the southwest.

Although portions of the Wildhorn Nappe folds may be described as either cylindrical or conical, the overall geometries are best described as periclinal, with hinge lines that plunge in both directions from a central culmination and curve away from the regional strike towards the lateral terminations. This periclinal geometry is demonstrated in two ways. The first is through hinge point tie lines in map view. Hinge points are locations where a fold hinge line passes through the topographic surface, and straight lines which connect hinge points at the same stratigraphic level within the same fold are hinge point tie lines (Ramsay 1989). Such lines facilitate analysis of regional fold hinge trends, and Ramsay (1989) has used them to demonstrate the consistent and parallel fold trends in the western Helvetics. The hinge point tie lines for folds 3 B and 5 (Fig. 9), however, show a progressive curvature away from the average strike direction as the fold terminations are approached. Near the culminations, the tie line trends average 055°, but to the northeast they reach 070°, and to the southwest they trend 045°. The parallelism of the hinge point tie lines for the two folds suggests that the patterns may be due to slight regional bending or folding of the entire Wildhorn Nappe. However, as other folds have different trends (Fig. 8), it is more probable that it simply results from two folds initiating in close proximity to each other and undergoing similar growth and amplification during progressive simple shear.

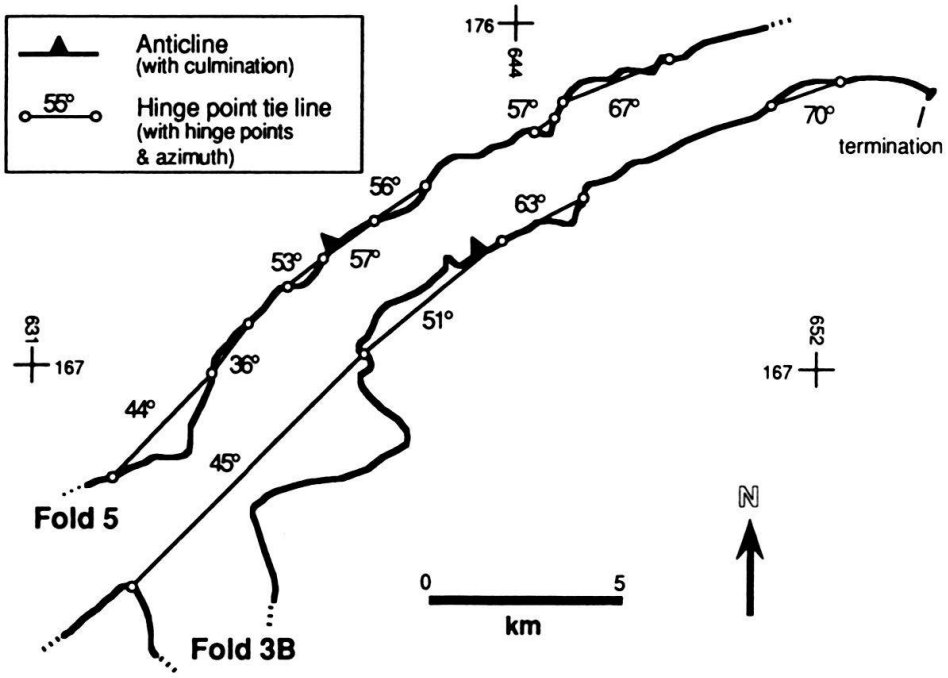

Fig. 9. Map view of hinge lines for folds 3 B and 5. Hinge point tie lines (see text) show curving nature of hinges as fold terminations are approached.

The second method of depicting periclinal geometries is through axial plane diagrams. The mean axial plane orientation for a given fold is first determined by constructing lines joining all combinations of hinge line points for that fold, and finding the best-fit plane defined by these lines. Hinge line points for each formation are then plotted on the axial plane diagram and joined: the result is the trace of hinge lines in the axial plane, i.e. the intersections of folded bedding with the axial plane. The plots for folds 3B and 5 (Fig. 10) clearly show the doubly-plunging nature of the fold hinges. The geometries for both folds are similar, with approximately symmetrical plunges on either side of the culminations. The hinge lines pitch 12° and 14° in the axial planes, equivalent to true plunges of about 7°.

Periclinal fold geometries by definition require axial extension to accommodate hinge line lengthening (DeSitter 1956, Ratliff 1992). Evidence for true axial extension (dilatant veins, pressure fringes) has been noted from many folds (e.g., Cloos 1947, Nickelsen 1966, Ramsay 1981) and is distinguished from apparent axial extension caused by, for example, superposition of compactional and tectonic strains (Ramsay 1967). The Wildhorn Nappe folds contain common dilatant veins oriented roughly perpendicular to fold axes. With rare exceptions, these veins formed during fold development, as indicated by mutual cross-cutting relationships with both profile-plane veins and solution cleavage resulting from fold amplification and rotation (Rowan & Kligfield 1992). Thus, these veins do not represent the late axial-parallel extension documented in other parts of the Helvetics (Durney & Ramsay 1973, Dietrich & Durney 1986, Burkhard 1986) and ascribed to either a change in direction of overthrust shear (Dietrich & Casey 1989, Dietrich 1989a, 1989b) or development of the major Helvetic culminations and depressions (Sanderson 1982, Burkhard 1986, Ramsay 1989). Instead, they are a manifestation of axial-parallel extensional strains related to the folding process itself. There is some

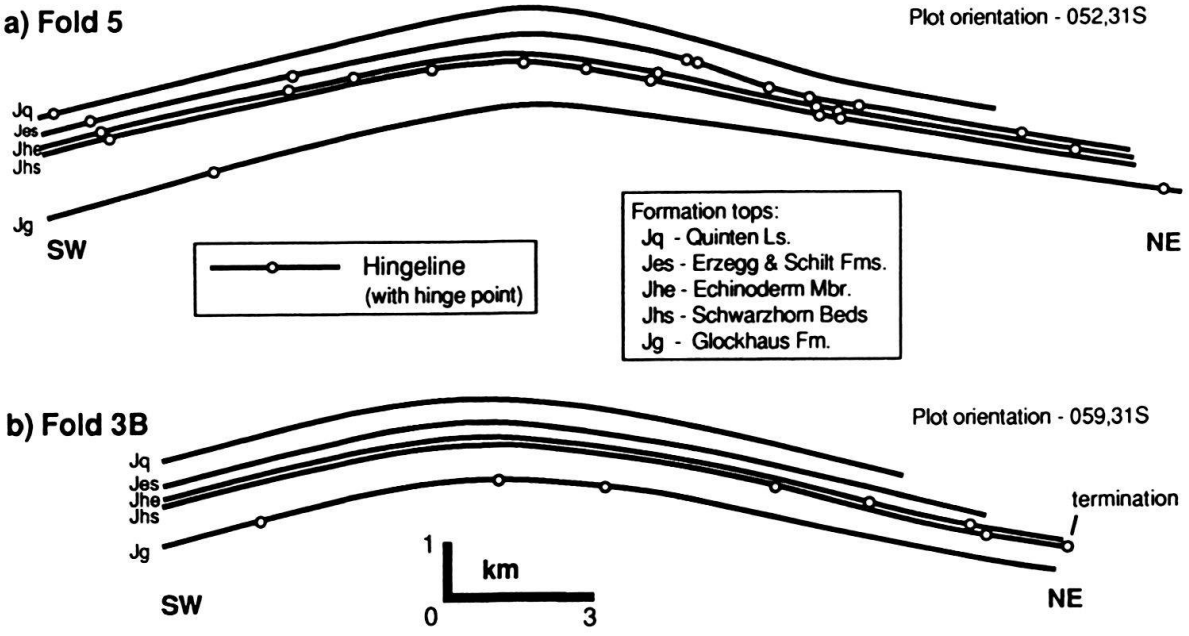

Fig. 10. Axial plane plots showing longitudinal geometries of: a) fold 5, and b) fold 3B. Hingelines are doubly-plunging away from fold culminations. The angle from horizontal is the pitch in the axial plane, not the true plunge (see text).

evidence for late-stage extension, in the form of very rare axial-perpendicular dilatant veins which have moderate dips (40–60° SW or NE) and which postdate all other features. These account for less than 1% extension, in contrast to the 5–15% late axial extension reported by Burkhard (1986). The disparity may be explained partly by variations in regional plunge: the area of this investigation lies near the culmination of the Aar massif, whereas Burkhard studied the southwestern termination, where the Helvetic nappes plunge up to 25°. Pfiffner (1981 a) recorded up to 25% apparent extension on the Vättis culmination of the eastern Aar massif, but this may not represent true axial stretching because of, e.g., possible volume loss strain.

In a simple model in which a fold hinge line originates as a straight line linking the two points in undeformed bedding which eventually become the fold terminations, axial extension (in percent) at any location is equal to $(1/\cos \omega\text{-}1) * 100$, where ω is the local hinge line pitch in the axial plane. More complicated models, for example with the hinge line originating as a curved line, may be more appropriate, but should create only small departures from the relationship given above. In any case, axial extensions should increase with increasing pitch, and should be greatest at the hinges and decrease in magnitude down-dip on the limbs (DeSitter 1956). The axial extensions recorded by dilatant veins were measured at 17 sites along folds 3B and 5 (Rowan 1991, Rowan et al. 1991), and are plotted in Fig. 11 against the local axial plunge, measured as the pitch in the axial plane. Although the data do not fit the $1/\cos \omega$ curve precisely, there is a clear correlation between increasing pitch and axial extension, providing further evidence that the axial extension is an integral component of fold growth and amplification.

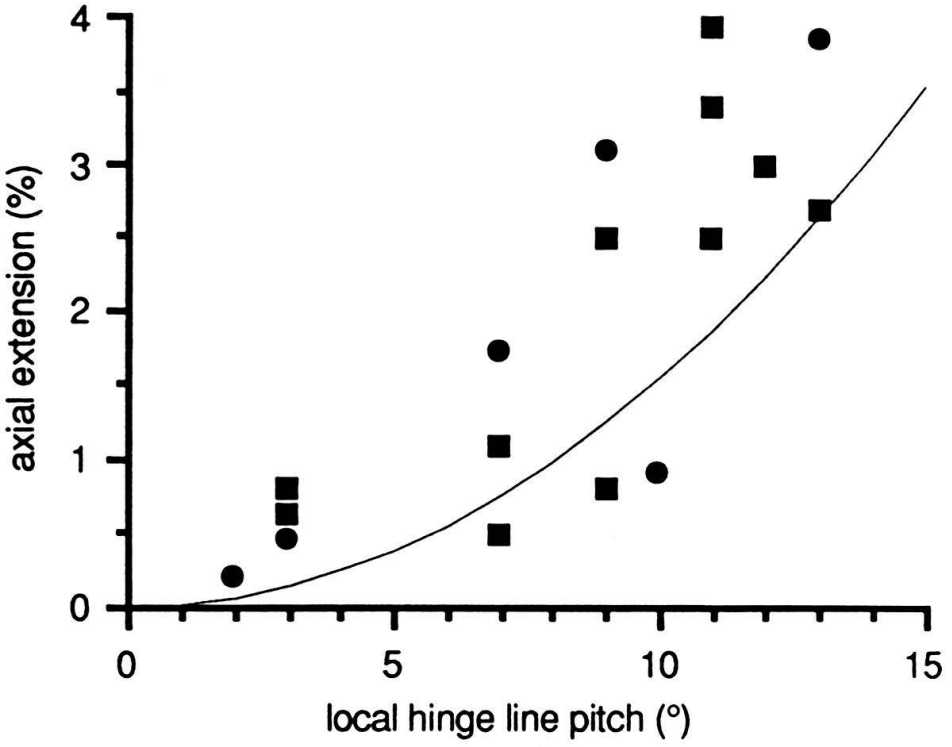

Fig. 11. Plot of measured axial-parallel extension versus the local axial plunge (calculated as the pitch in the axial plane). Squares are data points from the southwestern halves of the folds, circles are from the northeastern halves. The curve shows the expected extensions if they are inversely proportional to the cosine of the pitch (see text).

The data in Fig. 11 show that there is no difference in axial extension between the northeastern and southwestern halves of the folds. This suggests, but does not necessitate, that shortening and the nappe transport direction were both essentially perpendicular to the average fold strike. If the folds had formed in a zone oblique to the transport direction, the extension data might be expected to be distributed asymmetrically.

Faults

Both thrust and normal faults of all scales are found in the study area. These are described in the sections below, and several examples are discussed in detail.

Thrust faults

Thrust faults within the Wildhorn Nappe are surprisingly uncommon considering the compressional tectonic setting. At one end of the scale, small contractional wedge faults are very rare. These are usually interpreted as early features accommodating initial layer-parallel shortening (e.g., Mitra et al. 1984), and their scarcity here is attributed to the mechanical stratigraphy. Contractional wedge faults generally form in thrust belts dominated by small ductility contrasts and low ratios of incompetent to competent layer thicknesses, in which early layer-parallel compression results in internal shortening and thickening (Ramsay & Huber 1987, p. 418). In the Wildhorn Nappe, however, early layer-parallel shortening is accommodated almost immediately by buckling and sideways deflection of the Jurassic multilayer into the adjacent thick incompetent formations (Rowan & Kligfield 1992).

Larger thrust faults with ramps underlying the major folds appear to be nonexistent. Although such thrusts would be expected according to the fault-bend and fault-propagation fold models (e.g., Suppe 1985), the two deep profiles, in the Lütschine valleys in the southwestern half and along the Aare Valley at the northeastern margin, show no evidence for fault ramps at the cores of any of the folds. This observation and the fold geometries clearly indicate that the dominant style is that of detachment folding, and that fault-bend and fault-propagation fold models are inappropriate for at least this portion of the Wildhorn Nappe.

Three major thrust faults have been mapped in the area, and all appear to be related to synclinal space problems. Two formed as a response to tightening of the syncline below folds 3A/B/C, both to the southwest (sections A–A′ to C–C′) and to the northeast (section G–G′). Hinge collapse at the level of the Dogger formations created isoclinal geometries (Fig. 6c), leaving no room for higher units in the fold core. The Quinten Limestone therefore detached and was thrust out over the normal limbs, using the weak Erzegg/Schilt marls as a glide plane. This style, which represents a departure from the normal harmonic fold geometries, does not appear to be continuous through the center of the area, as no syncline tightening and associated thrusting is visible on the north slope of the Schwarze Lütschine Valley (section D–D′), and the northeastern fault probably dies out between sections G–G′ and F–F′.

The third major thrust occurs along the southeastern margin of the area adjacent to the nappe boundary with the Aar massif (Fig. 2). It is consistent feature, occurring in all sections except G–G′, and has variable displacements of up to over 1 km. It dips 35–40° SE in sections E–E′ and F–F′, but changes to lower, and even northwest, dips

to the southwest, coincident with the overall tilting of the nappe in this area (e.g., section A–A′). Although the hanging wall is usually a normal limb with upright dips, the fault cuts variably through the folded nappe: a major overturned syncline is in the immediate hanging wall in section A–A′, and fold 2A in the footwall is truncated by the fault in the vicinity of section D–D′. Because of these observations and the location of the fault just in front of the vertical portion of the basal detachment, it is interpreted as a relatively late feature that formed as an out-of-the-synform thrust during the folding of the entire nappe caused by the emplacement of the Aar massif.

Although the structure of this fault and its hanging wall and footwall is relatively simple in the vicinity of Grosse Scheidegg, the area around the Schilthorn and Birg is more complicated (Figs. 12, 13). The presence of isolated blocks of Quinten Limestone more than 1 km southeast of any equivalent coherent outcrops at the same structural level led Stauffer (1921, sections III, IV, V) to postulate the existence of a refolded isoclinal syncline, with small pods of limestone completely cut off from the main synclinal closure 1–2 km away along the axial plane. This interpretation is incompatible with both the observed field relationships and the known structural style. Instead, the blocks of Quinten Limestone, as well as blocks containing other lithologies, are interpreted as small horses along the fault plane (Fig. 13). This is supported by the presence of thin, sheared-out tails of Quinten Limestone along the fault plane below the Schilthorn (Fig. 12, grid reference 629.95, 156.1 and 631.0, 156.15).

At first glance, there are two apparent problems with this interpretation. First, it does not obviously explain the isolated nature of the blocks and the thrusting of younger over older units. Second, there is an apparent mismatch of hanging- and footwall flats, such that the section would not restore to a valid pre-faulting geometry. The footwall has a long flat in the Erzegg/Schilt Formations with no hanging wall counterpart, and the hanging wall has a long flat in the Quinten Limestone, as indicated by fault klippen of Quinten Limestone farther northwest (e.g., the Lobhörner, Fig. 2, grid reference 631.0, 161.3). Both problems are resolved by the model in Fig. 14, in which the horses are plucked from the hanging wall and possibly the footwall of a fault which ramps up through the already folded Dogger units, runs along the Erzegg/Schilt marls, and then ramps up through the Quinten Limestone. This interpretation also explains the anomalous presence of the Echinoderm Member at the top of Männlichen (Fig. 2, grid reference 638.25, 163.1), where it is in thrust contact with underlying Erzegg/Schilt marls, and is partly overriden by Glockhaus shales (Section C–C′).

Normal faults

The Wildhorn Nappe is characterized by common normal faults of all scales. Their origins, whether synsedimentary or syntectonic, are a matter of dispute. Günzler-Seiffert (1941 a) first noted the presence of these faults and proposed that they were the result of an early extensional deformation and were later modified or reactivated during Alpine compression, an interpretation that has been followed by Pilloud (1990). Certainly, early (Triassic-Jurassic) normal faults are well documented in other portions of the Alps (e.g., Lemoine et al. 1986, Lemoine & Trümpy 1987, Gillcrist et al. 1987, Froitzheim 1988). However, most of the normal faults in the studied portion of the Wildhorn Nappe are confined to backlimbs, and some even offset fold axial planes (for example, faults on fold

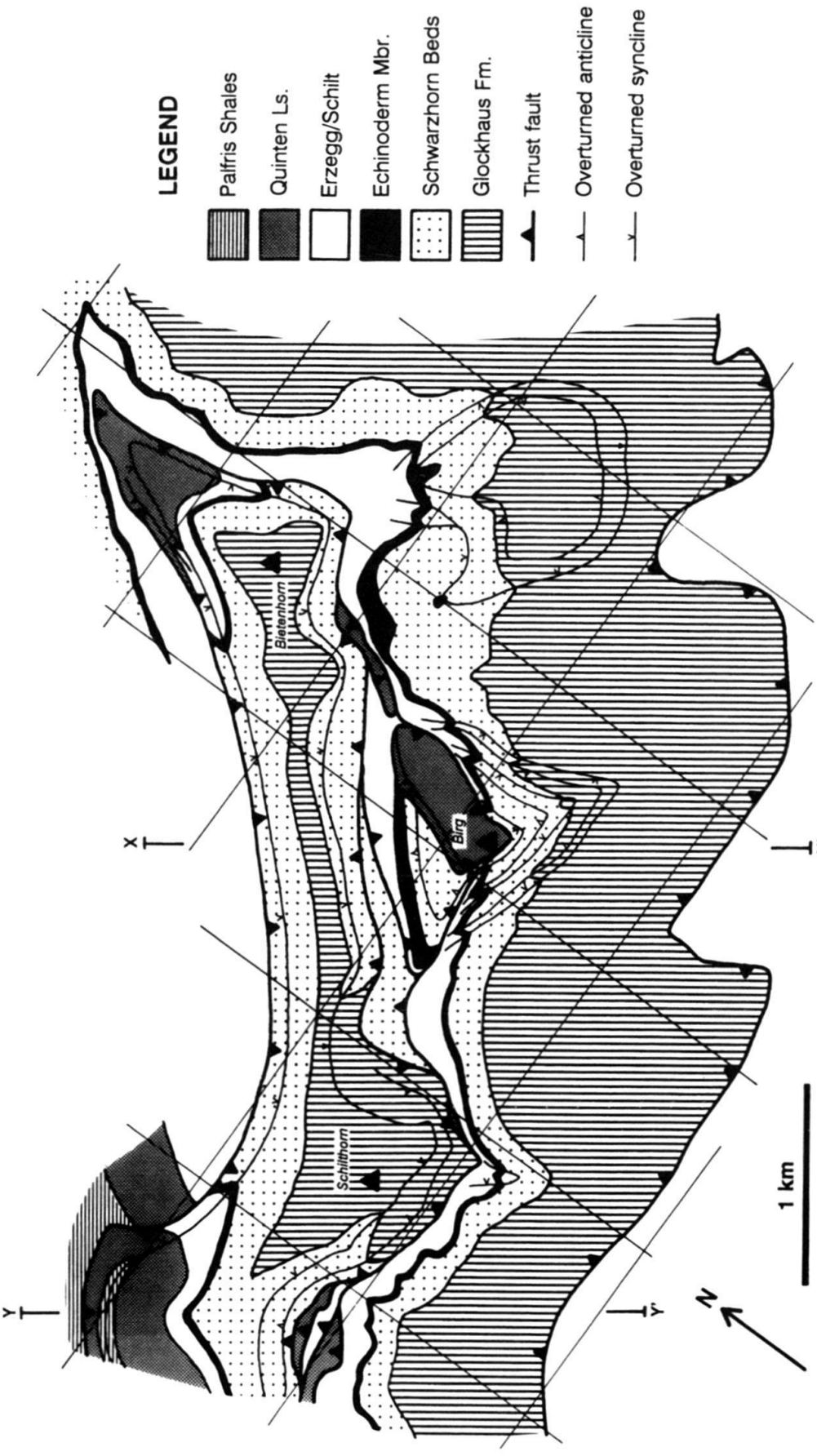

Fig. 12. Detailed geologic map of the Schilthorn area showing thrust-fault klippe and isolated horses along fault surface. Cross sections X – X′ and Y – Y′ shown in Fig. 13.

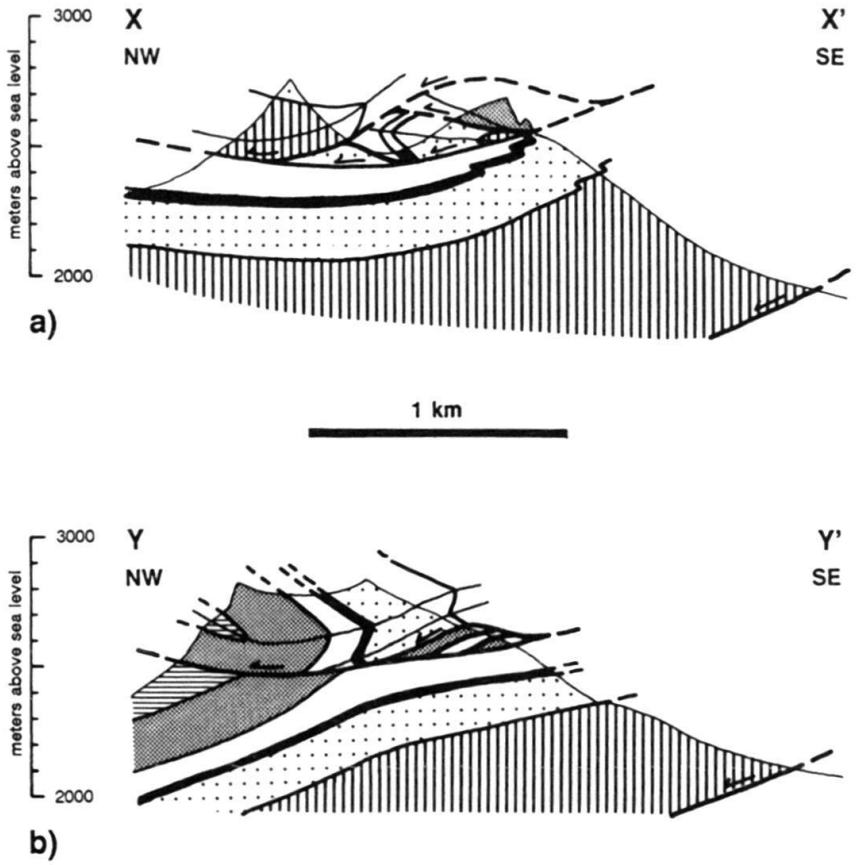

Fig. 13. Cross sections through Schilthorn area (see Fig. 12 for locations), showing varied nature of horses along thrust surface. See Fig. 12 for key to patterns.

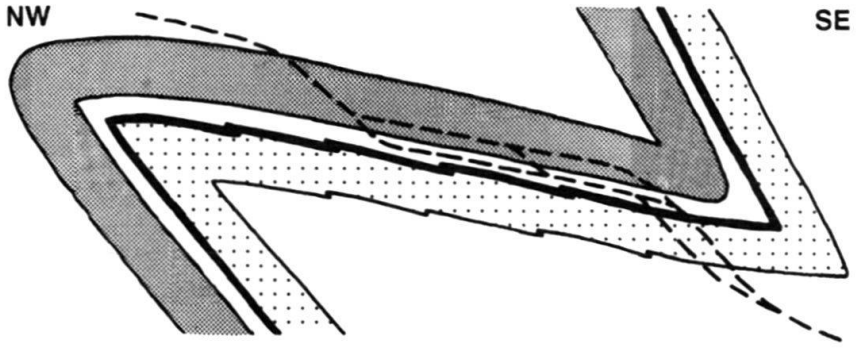

Fig. 14. Proposed pre-thrusting geometry for the Schilthorn area, with horses originating as fault-bounded slivers peeled from hanging wall and footwall. Future trajectory of faults indicated by dashed lines.

5 in sections C–C′ and E–E′). Many of the faults are thus clearly syntectonic, and may be similar to those described by Ramsay et al. (1983), who suggested that the faults developed when fold limbs rotated during simple shear into orientations which favor extension.

Not all of the faults, however, can be ascribed to syntectonic origins. One example of an early normal fault is found on the northern slope of the Schwarze Lütschine Valley (Fig. 2, grid reference 637.0–638.5, 165.7–166.4). Here a complicated zone is interpreted as a synsedimentary normal fault, striking roughly east-west and dipping to the south, that has placed Palfris Shales adjacent to the Quinten Limestone and has subsequently been folded in two anticlines and the intervening syncline. Many other small normal faults are clearly synsedimentary, as shown by stratigraphic thickness and facies changes across the faults. These have been documented within the study area by Pilloud (1990) and to the northwest by Herb (1988).

Although many of the small normal faults probably predate the folding, the origin of the two largest normal faults, cited by both Günzler-Seiffert (1941 a) and Pilloud (1990) as the best examples of synsedimentary faults, is problematic. These are the Sylere and Bürgle faults, which are found just to the northwest of fold 5 bounding an elongate horse dominated by an overturned limb containing the complete multilayer sequence. The faults have variable dips of between 65° SE and 85° NW, displacements of up to more than 1 km, and cut through the entire Jurassic portion of the nappe. The extensional horse is best seen on either side of the Lütschine Valley (sections B–B′ and C–C′), but can also be observed above Werzisboden (section E–E′, Fig. 2, grid reference 640.8, 171.4). The overturned limb often has an anticline and small normal limb at the top, and a similar syncline and normal limb at the bottom. Its footwall is the gently-dipping backlimb of the rounded fold 7 A or 7 B, and its hanging wall is formed by the forelimb of fold 5. The faults apparently continue over 10 km to the southwest into the Kiental (Günzler-Seiffert 1941 a, Pilloud 1990), and although they are mapped here to die out between sections E–E′ and F–F′, Pilloud (1990) suggests that they continue into the deeply-cut Giessbach Valley (grid reference 645, 173–175). In any case, they certainly are not present on the slopes of the Aare Valley just to the northeast. The presence of a single fault strand in the vicinity of section D–D′ shows that the faults merge upwards in the Cretaceous shales, and the faults are assumed to merge at depth with the basal detachment.

The extensional horse is associated with greater than normal deformation. First, the adjacent overturned limb of fold 5, although of normal thickness to the southwest, is substantially thinned to the northeast in the area of sections D–D′ and E–E′, with both the Echinoderm Member and the Quinten Limestone attaining approximately 50% of their normal nearby thicknesses. The Quinten Limestone can also be locally thinned in the overturned limb of the horse itself, although it is usually of normal thickness and relatively undeformed. Fig. 15 a is a sketch of the top of the horse in the Schynige Platte area, where a thinned Quinten Limestone is bounded by the two faults. Not only is the main overturned limb thinned, but the backlimb in the immediate footwall of the right-hand fault (location A) is extremely thin and characterized by an intense bedding-parallel pressure solution which presumably accommodates the thinning. Along the right-hand fault itself is a zone 2–4 m wide of intensely sheared Quinten Limestone (location B), consisting of wavy shale separating lenses of limestone marked by abundant bedding-parallel pressure solution and bedding-perpendicular veins producing down-dip extension (Fig. 15 b). The shale is interpreted as the insoluble residue left after dissolution of the vast majority of the carbonate component. In effect, this zone appears as a sheared and incredibly thinned and extended normal limb of Quinten Limestone.

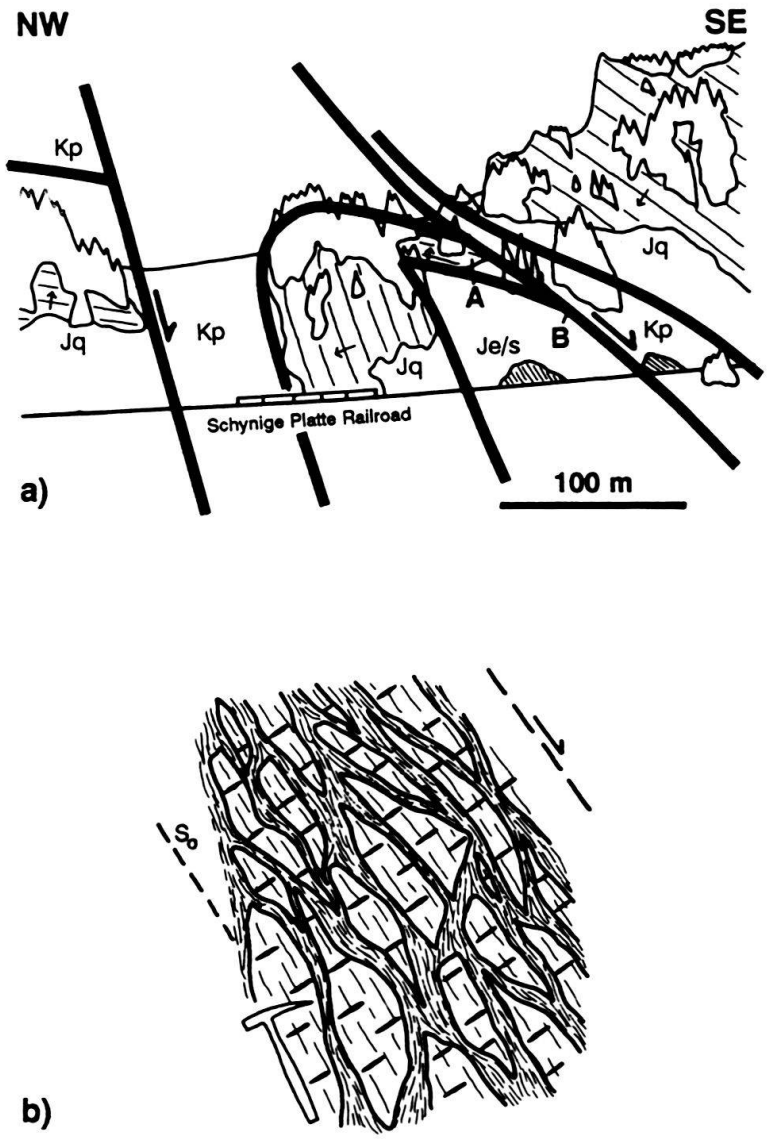

Fig. 15. a) Sketch of anticline with thinned backlimb at the top of the extensional horse near Schynige Platte. View to NE at grid reference 635.6, 167.25. Areas of outcrop are indicated by areas with thin lines showing bedding. Kp – Palfris Shales, Jq – Quinten Limestone, Je/s – Erzegg/Schilt Formations. Locations (A) and (B) are discussed in text. b) Detail from location (B), showing lenticular pods of Quinten Limestone separated by shales with shear textures. Within pods, solution cleavage (thin lines parallel to bedding – S_0) and extensional veins (gashes perpendicular to bedding) are shown diagramatically.

The origin of the extensional horse is uncertain, and five possible explanations are presented:

1) The faults could be early extensional features as proposed by Günzler-Seiffert (1941 a) and Pilloud (1990). In this model (Fig. 16 a), extension along southeast-dipping faults created offsets of essentially planar Jurassic beds, and Alpine compression and thrusting then modified this geometry by forming major folds and minor drag folds along the faults. This explanation is improbable because the current orientations of the faults are incompatible with original southeast dips. The Jurassic portion of the Wildhorn Nappe has been subjected to northwest-directed overthrust shear, with a

shear strain (γ) of close to 3, which has caused significant rotation of bedding, fold axial planes, and presumably any early faults (Rowan & Kligfield 1992). A fault with an original 70° dip to the southeast would now have shallow southeasterly dips (less than 20°), as opposed to the 65° SE to 85° NW dips observed. Even if the simple shear model is an over-simplification of the true kinematic development, it is difficult to envision how southeast-dipping normal faults could end up with local northwest dips in an environment of northwest-directed overthrust shear. In addition, the restoration of section D–D′ (Fig. 5) provides further evidence that the faults originally dipped to the northwest. If they had original southeast dips similar to their current orientations, as suggested by Günzler-Seiffert (1941 a) and Pilloud (1990), they could be used as rough pin lines in the restoration, a scenario which would require a distribution of flexural slip incompatible with that observed (Rowan 1991).

2) The faults could be late features which post-date the compressional deformation. This possibility is discounted because of the intense deformation associated with the horse, the lack of a suitable tectonic event to explain such deformation, and the requirement of a long, anomalous forelimb in the pre-faulting geometry (Fig. 16 b). This interpretation would also require that the basal detachment of the Wildhorn Nappe is offset, for which there is no evidence one way or the other.
3) The faults could be normal faults that developed during the compressional deformation. In this scenario, they would have a similar origin to the smaller normal faults and those noted by Ramsay et al. (1983), being large examples of extension along normal limbs oriented parallel to the extensional field of the nappe-bounded shear couple (Fig. 16 c). Although this is compatible with the thinned and extended sliver of Quinten Limestone along one of the faults (Fig. 15), there are several problems. First, there is nothing unusual in the stratigraphy or structural orientations to explain why these limbs extended in such a manner when all other backlimbs are relatively undeformed. Second, the localized steep, even northwesterly, dips of the faults are incompatible with this model, as they are not in the proper orientation for extension, and removing any rotation caused by simple shear only exacerbates the problem.
4) The faults could have originated as northwest-dipping back-thrusts that formed in response to early compression. Subsequent northwest-directed overthrust shear would have then rotated and modified the thrusts into their current orientations and apparent normal offsets (Fig. 16 d). This model is also compatible with the thinned Quinten Limestone sliver, and has the added advantage of best explaining the current dips of the faults. Present-day dips of 65° SE to 85° NW would have had original dips of close to 20° NW prior to rotation in overthrust simple shear (see Rowan & Kligfield 1992), a model supported by the restoration in Fig. 5. Furthermore, the sigmoidal shape of the faults, with steeper dips in the middle, is compatible with the observations of increased simple shear close to the bounding detachments (Ramsay 1981, Casey & Huggenberger 1985, Dietrich & Casey 1989). However, there is again the problem of why this type of deformation is not found elsewhere. More importantly, the postulated thrust faults are incompatible with the observed lack of other such features as a response to early layer-parallel compression, and with the known ductility contrasts and ratios of incompetent to competent layer thicknesses. Finally, in northwest-directed overthrust shear, thrust faults with northwest dips would not be expected to develop, unless they represent preexisting northwest-dipping normal

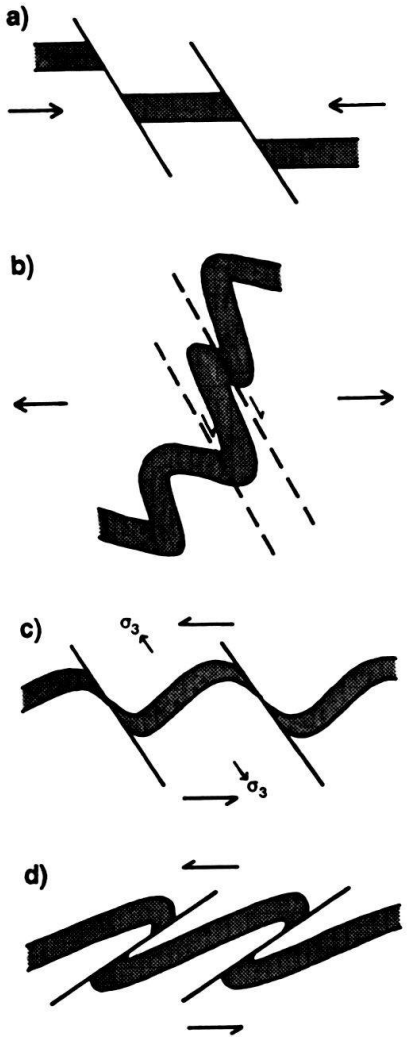

Fig. 16. Different models for origin of faults bounding the extensional horse (see text): a) pre-tectonic normal faults; b) post-tectonic normal faults; c) syn-tectonic normal faults; and d) early back-thrusts. Large arrows indicate subsequent compression in (a), subsequent extension in (b), and orientation of nappe simple shear in (c) and (d), and σ_3 is minimum principal compressive stress.

faults. Another possibility that must be considered is that they formed in response to early pure-shear compression caused by buttressing against a large normal fault located to the northwest (e.g., Lemoine et al. 1986, Gillcrist et al. 1987).

5) The faults could be strike-slip faults so that the horse is part of an overturned fold limb emplaced in its current location by lateral movement. However, the observed termination of the faults within the field area implies that any strike-slip component, if present, must be minimal, and this model is thus incapable of fully explaining the origin of the extensional horse.

Although none of the models adequately explains the observed geometries and deformation, the early backthrust interpretation best explains the current orientations of the fault planes. Nevertheless, the reasons for the localized expression of this structural style are unclear, and a more thorough investigation is required to address these issues.

Other faults

One other type of fault is found in the area. These are low displacement, flat to northwest-dipping detachments which carry blocks of Quinten Limestone in their hanging walls. They are found on the Schwabhorn (Fig. 2, grid reference 642.15, 170.4; section E–E′) and the Oltschiburg (grid reference 648.95, 174.1), and are interpreted as relatively recent features along which isolated masses of Quinten Limestone from the fold 5 forelimb have slid a short distance down the topographic slope (Fig. 17). Alternatively, they may be somehow related to the emplacement of the Aar massif and folding of the Wildhorn Nappe. In either case, they are younger than the main deformation phase which created the folds.

It is emphasized that the Quinten Limestone geometries observed at Oltschiburg are atypical, as are those found in the Schilthorn area. In these regions, the Quinten Limestone appears to deform in a manner unlike that of deeper levels. However, the Quinten Limestone and the Dogger units form harmonic folds throughout the majority of the study area, as the intervening incompetent Schilt and Erzegg Formations are not thick enough to accommodate separate and distinct fold geometries above and below. This is not to say, however, that these latter units cannot form detachments, as the geometric problems created by overtightening of synclines at Dogger levels are resolved by thrusting along the Schilt/Erzegg marls.

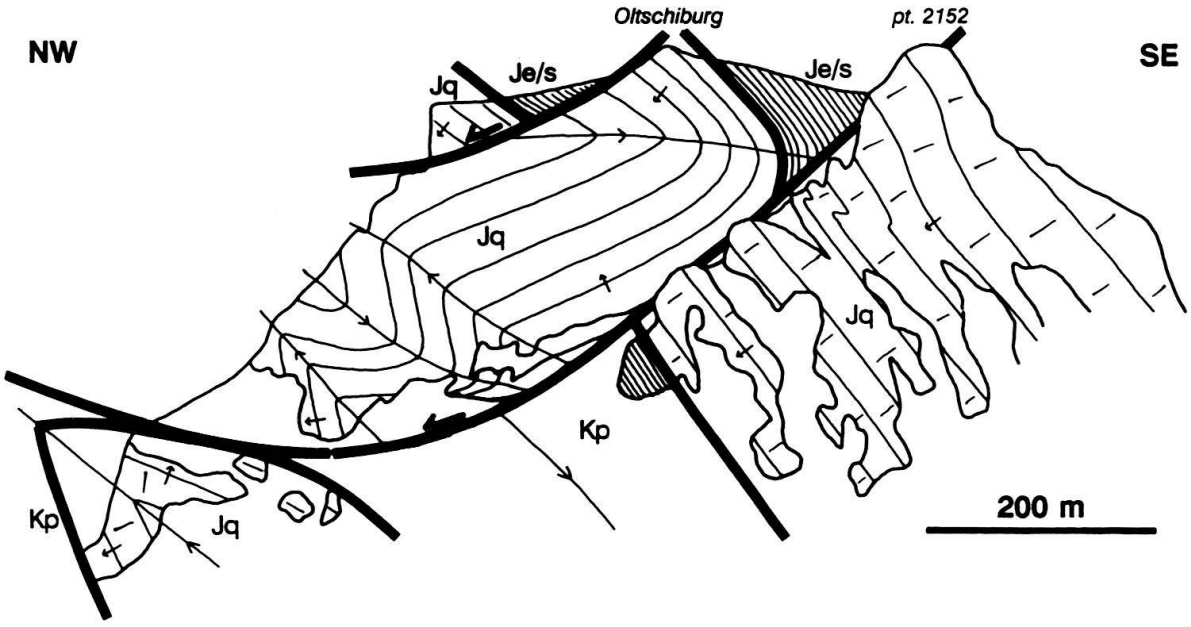

Fig. 17. Sketch of SW face of Oltschiburg (grid reference 648.7, 174.1). Two post-tectonic, gravity-driven faults displace portions of the forelimb of fold 5. Medium-scale parasitic faults in hanging wall of lower fault and major syncline in footwall are cut by the fault. The frontal (NW) overturned limb in the hanging wall probably corresponds to the footwall forelimb. Displacement is about 150 m on upper fault, and probably about 600 m on lower fault. A similar fault is visible in the same structural position 7.5 km SW on the Schwabhorn, but not on the intervening Axalphorn or Tschingel.

Discussion and conclusions

The geometries presented in this report for the Jurassic portion of the Wildhorn Nappe are different in many respects from those that have been accepted for many years. Specifically, the cross sections (Fig. 4) deviate markedly from those of Stauffer (1921), Günzler-Seiffert (1934b, 1967), and Pilloud (1982, 1990). Although there are undoubtedly instances in which the other sections are more accurate, especially in depicting some of the small-scale details, they often contain significant errors in some of the large-scale structures. Most of the discrepancies can be attributed to the enormous advances over the years in our understanding of the origin and geometries of thrust nappes and their associated folds. Factors that have explicitly been considered in constructing the cross sections presented here include: models of buckled multilayers and the influence of layer thicknesses and competencies (e.g., Ramberg 1970a, b, Ramsay & Huber 1987); cross section restoration and balancing and the concepts of retrodeformation (Suppe 1985) and kinematic admissibility (Geiser 1988); and large-scale three-dimensional strain compatibility, including models of displacement variation (e.g., Chapman & Williams 1984). Other discrepancies can be attributed to differences in correlation of structural elements and projection of data into cross sections. Finally, in areas of relatively poor exposure (e.g., the wooded slope above the Brienzer See), the geometries are drawn here in a fashion similar to that observed where exposure is better. This contrasts with other sections which often show complex structures in such areas (e.g., Pilloud 1990).

There are numerous examples of geometries in previous interpretations which are considered incorrect for the reasons mentioned above. Firstly, the old sections sometimes show major disharmony between the Quinten Limestone and the underlying Hochstollen and Glockhaus Formations. Yet, as discussed above, the entire stratigraphic sequence from the Quinten Limestone down to the Glockhaus Formation generally acts a single multilayer that formed harmonic buckle folds (except where synclines have been overtightened). Secondly, restorations of many of the interpretations would yield totally unacceptable undeformed geometries. One unpublished section (profile 4 through the eastern Faulhorn Group) by Günzler-Seiffert, for example, shows a ratio of Quinten Limestone to Echinoderm Member bed lengths of greater than 1.5:1. Thirdly, an area of interlocking 'hooks' of Quinten Limestone (Günzler-Seiffert 1934b, Fig. 2, Pr. 5&7) is kinematically impossible. Fourthly, the thrusted limb of fold 4B in the extreme northeast (section G–G′) was interpreted as a separate structure which was projected under the fold in adjacent structures (Pilloud 1982, fold 5o). Fifthly, the thrust fault below fold 3C (sections B–B′ and C–C′) was miscorrelated so that what is in reality a continuous syncline was placed in the hanging wall in one section (Günzler-Seiffert, unpublished) and the footwall in an adjacent section (Stauffer 1921). And finally, a fault changes from reverse displacement of 450 m to a normal displacement of 100 m between adjacent cross sections only 800 m apart (Pilloud 1990, Figs. 13c, d, fault between folds 3m&3u).

It is stressed that the Wildhorn Nappe folds are demonstrably detachment folds with cores of incompetent material rather than structures with underlying thrust ramps, such as fault-bend or fault-propagation folds. These latter models may be adequate approximations in stratigraphic sequences with relatively low ductility contrasts and low ratios of incompetent to competent rocks, but their application to sequences such as those found in this portion of the Helvetic nappes is inappropriate.

In three dimensions, the fold shapes are periclinal rather than cylindrical, with hinge lines that curve and plunge away from central culminations. Although the regional fold trends may be parallel (Ramsay 1989), in detail each fold hinge line varies over 20° in trend from one end of the fold to the other. The overall pattern is very similar to that produced experimentally by Dubey & Cobbold (1977). In their models, buckle folds initiated and then amplified and propagated laterally with increasing compression. Fold hinges were curved and plunged rapidly at terminations, especially where propagating fold complexes interfered during growth. They also noted that culminations were characterized by chevron geometries, whereas terminations had more rounded fold geometries. This feature is not observed in the Wildhorn Nappe: although there are exceptions, folds often keep the overturned, chevron-like shapes (at the Echinoderm Member level) as they lose amplitude towards the terminations (e.g., fold 3A, Fig. 8). The difference possibly lies in the simple shear origin of the Helvetic folds as compared to the pure shear experimental models.

The overall development of the folds in the Wildhorn Nappe is visualized as being similar to the models of Dubey & Cobbold (1977). Overthrust shear first triggered the initiation of symmetric buckle folds (Rowan & Kligfield 1992), possibly at irregularities in the layering or stress field. These grew in amplitude and probably length with time, forming roughly parallel folds with hinges that curved and plunged towards the terminations, and were modified by continuing simple shear into their current asymmetric geometries.

Acknowledgments

Roy Kligfield is thanked for providing the opportunity to study these folds and for his overall guidance on the project, and Bob Ratliff's help in the field and many useful discussions are greatly appreciated. A. Pfiffner, M. Burkhard, and R. Herb provided thoughtful reviews of the manuscript, and A. Pfiffner is especially thanked for the German translation of the abstract. Finally, the friendship of T. Brunner in Lausanne and the hospitality and kindness of the Stalder family in Lütschental helped make two field seasons very enjoyable. The research was funded by NSF grant EAR 86-16640 to R. Kligfield.

REFERENCES

BURKHARD, M. 1986: Déformation des calcaires de l'Helvétique de la Suisse occidentale (Phénomènes, mécanismes et interprétations tectonique). Rev. Géol. dynam. Géogr. phys. 27, 281–301.

– 1988: L'Helvétique de la bordure occidentale du massif de l'Aar (évolution tectonique et métamorphique). Eclogae geol. Helv. 81, 63–114.

CASEY, M. & HUGGENBERGER, P. 1985: Numerical modelling of finite-amplitude similar folds developing under general deformation histories. J. Struct. Geol. 7, 103–114.

CHAPMAN, T. J. & WILLIAMS, J. D. 1984: Displacement-distance methods in the analysis of fold-thrust structures and linked-fault systems. J. Geol. Soc. London 141, 121–128.

CLOOS, E. 1947: Oolite deformation in the South Mountain fold, Maryland. Bull. Geol. Soc. Am. 58, 843–918.

DESITTER, L. U. 1956: The strain of rock in mountain building processes. Am. J. Sci. 254, 585–604.

DIETRICH, D. 1989a: Axial depressions and culminations in the evolution of the Helvetic chain. Schweiz. mineral. petrogr. Mitt. 69, 183–189.

– 1989b: Fold-axis parallel extension in an arcuate fold- and thrust belt: the case of the Helvetic nappes. Tectonophysics 170, 183–212.

DIETRICH, D. & CASEY, M. 1989: A new tectonic model for the Helvetic nappes. In: Alpine Tectonics (Ed. by COWARD, M. P., DIETRICH, D. & PARK, R. G.). Geol. Soc. London Spec. Pub. 45, 47–63.

DIETRICH, D. & DURNEY, D. W. 1986: Change of direction of overthrust shear in the Helvetic nappes of western Switzerland. J. Struct. Geol. 8, 389–398.

DUBEY, A. K. & COBBOLD, P. R. 1977: Noncylindrical flexural slip folds in nature and experiment. Tectonophysics 38, 223–239.

DURNEY, D. & RAMSAY, J. G. 1973: Incremental strains measured by syntectonic crystal growths. In: Gravity and Tectonics (Ed. by DEJONG, K. & SCHOLTEN, R.). Wiley, New York, 67–96.

FROITZHEIM, N. 1988: Synsedimentary and synorogenic normal faults within a thrust sheet of the Eastern Alps (Ortler zone, Graubünden, Switzerland). Eclogae geol. Helv. 81, 593–610.

GEISER, P. A. 1988: The role of kinematics in the construction and analysis of geological cross sections in deformed terranes. In: Geometries and Mechanisms of thrusting (Ed. by MITRA, G. & WOJTAL, S.). Geol. Soc. Am. Spec. Pap. 222, 47–76.

GILLCRIST, R., COWARD, M. P. & MUGNIER, J.-L. 1987: Structural inversion and its controls: examples from the Alpine foreland and the French Alps. Geodinamica Acta 1, 5–34.

GÜNZLER-SEIFFERT, H. 1925: Der geologische Bau der östlichen Faulhorngruppe im Berner Oberland. Eclogae geol. Helv. 19, 1–86.

– 1934a: Erläuterungen zu Blatt 395, Lauterbrunnen und nördl. Randgebiet v. Bl. 488 Blümlisalp, Atlasblatt 6 des Geol. Atlas d. Schweiz. Geol. komm. S.N.G., Bern.

– 1934b: Geologischer Führer der Schweiz: Fasc. IX, Centralschweiz, Exkursionen Nr. 45–52. Schweiz. Geol. Ges., Wepf & Co., Basel.

– 1941a: Persistente Brüche im Jura der Wildhorndecke des Berner Oberlandes. Eclogae geol. Helv. 34, 164–172.

– 1941b: Die Unterfläche der Wildhorndecke zwischen Kien und Aare. Eclogae geol. Helv. 34, 172–176.

– 1967: Geologischer Führer der Schweiz: Heft 4, Berner Jura (Basel-Neuchâtel-Biel), Berner Mittelland, Berner Oberland (ohne Grimsel, Brünig und Simmental), Exkursionen Nr. 13–18. Schweiz. Geol. Ges., Wepf & Co., Basel.

GÜNZLER-SEIFFERT, H. & WYSS, R. 1938: Erläuterungen zu Blatt 396, Grindelwald. Geol. Kommission S.N.G., Bern.

HEIM, A. 1921: Das helvetische Deckengebirge. Geologie der Schweiz, Bd. II. Tauchnitz, Leipzig.

HERB, R. 1988: Eocaene Paläogeographie und Paläotektonik des Helvetikums. Eclogae geol. Helv. 81, 611–657.

LANGENBERG, W., CHARLESWORTH, H. & LARIVIERE, A. 1987: Computer constructed cross sections of the Morcles nappe. Eclogae geol. Helv. 80, 655–667.

LEMOINE, M., BAS, T., ARNAUD-VANNEAU, A., ARNAUD, H., DUMONT, T., GIDON, M., BOURBON, M., DEGRACIANSKY, P.-C., RUDKIEWICZ, J.-L., MEGARD-GALLI, J. & TRICART, P. 1986: The continental margin of the Mesozoic Tethys in the western Alps. Mar. Pet. Geol. 3, 179–199.

LEMOINE, M. & TRÜMPY, R. 1987: Pre-oceanic rifting in the Alps. Tectonophysics 133, 305–320.

LUGEON, M. 1902: Les grandes nappes de recouvrement des Alpes du Chablais et de la Suisse. Bull. Soc. géol. Fr. 1, 723–825.

MARSHAK, S. & ENGELDER, T. 1985: Development of cleavage in limestones of a fold-thrust belt in eastern New York. J. Struct. Geol. 7, 345–359.

MASSON, H., HERB, R. & STECK, A. 1980: Helvetic Alps of western Switzerland. Excursion I. In: Geology of Switzerland, a Guide Book. Part B, Geological excursions (Ed. by TRÜMPY, R.). Wepf & Co., Basel, 109–145.

MITRA, G., YONKEE, W. A. & GENTRY, D. J. 1984: Solution cleavage and its relationship to major structures in the Idaho-Utah-Wyoming thrust belt. Geology 12, 354–358.

NICKELSEN, R. P. 1966: Fossil distortion and penetrative rock deformation in the Appalachian Plateau, Pennsylvania. J. Geol. 74, 924–931.

PFIFFNER, O. A. 1978: Der Falten- und Kleindeckenbau im Infrahelvetikum der Ostschweiz. Eclogae geol. Helv. 71, 61–84.

– 1981a: Strain analysis in folds (Infrahelvetic complex, Central Alps). Tectonophysics 61, 337–362.

– 1981b: Fold-and-thrust tectonics in the Helvetic Nappes (E. Switzerland). In: Thrust and Nappe Tectonics (Ed. by MCCLAY, K. R. & PRICE, N. J.). Geol. Soc. London Spec. Pub. 9, 319–327.

PILLOUD, A. 1982: Geologie im Gebiet der Axalp (Faulhorn-Gruppe). Liz. Univ. Bern (unpublished).

– 1990: Bau und Jurassische Präorogene Tektonik der Helvetischen Hauptschubmasse im Berner Oberland. Unpublished Ph.D. Thesis, Univ. Bern.

RAMBERG, H. 1970a: Folding of laterally compressed multilayers in the field of gravity, I. Phys. Earth Planet. Interiors 2, 203–232.

– 1970 b: Folding of laterally compressed multilayers in the field of gravity, II: numerical examples. Phys. Earth Planet. Interiors 4, 83–120.

RAMSAY, J. G. 1967: Folding and Fracturing of Rocks. McGraw-Hill, New York.

– 1981: Tectonics of the Helvetic nappes. In: Thrust and Nappe Tectonics (Ed. by MCCLAY, K. R. & PRICE, N. J.). Geol. Soc. London Spec. Pub. 9, 293–309.

– 1982: Rock ductility and its influence on the development of tectonic structures in mountain belts. In: Mountain Building Processes (Ed. by HSÜ, K.). Academic Press, London, 111–127.

– 1989: Fold and fault geometry in the western Helvetic nappes of Switzerland and France and its implication for the evolution of the arc of the western Alps. In: Alpine Tectonics (Ed. by COWARD, M. P., DIETRICH, D. & PARK, R. G.). Geol. Soc. London Spec. Pub. 45, 33–45.

RAMSAY, J. G., CASEY, M. & KLIGFIELD, R. 1983: Role of shear in development of the Helvetic fold-thrust belt of Switzerland. Geology 11, 439–442.

RAMSAY, J. G. & HUBER, M. I. 1987: The Techniques of Modern Structural Geology, v. 2, Folds and Fractures. Academic Press, London.

RATLIFF, R. A. 1992: Deformation studies of folding and faulting: cross section kinematics, strain analysis, and three-dimensional geometry. Unpublished Ph.D. thesis, University of Colorado, Boulder.

ROWAN, M. G. 1991: Geometry, kinematics, and strain partitioning of large-scale asymmetric buckle folds from the Wildhorn Nappe, Switzerland. Unpublished Ph.D. thesis, University of Colorado, Boulder.

ROWAN, M. G. & KLIGFIELD, R. 1992: Kinematics of large-scale asymmetric buckle folds in overthrust shear: an example from the Helvetic nappes. In: Thrust Tectonics (Ed. by MCCLAY, K. R.). Chapman & Hall, London, 165–173.

ROWAN, M. G., KLIGFIELD, R. & ERSLEV, E. A. 1991: Volume flux during folding in the Helvetic nappes, Switzerland. Geology 19, 1001–1004.

SANDERSON, D. J. 1982: Models of strain paths and strain fields within nappes and thrust sheets. Tectonophysics 88, 201–233.

STAUFFER, H. 1921: Geologische Untersuchung der Schilthorngruppe im Berner Oberland. Unpublished Ph.D. thesis, Universität Bern, Switzerland.

SUPPE, J. 1985: Principles of Structural Geology. Prentice-Hall, New Jersey.

TRÜMPY, R. 1969: Die helvetischen Decken der Ostschweiz: Versuch einer palinspastischen Korrelation und Ansätze zu einer kinematischen Analyse. Eclogae geol. Helv. 62, 105–142.

– 1980: An outline of the geology of Switzerland. In: Geology of Switzerland, a Guide Book (Ed. by TRÜMPY, R.). Wepf & Co., Basel, 1–104.

Manuscript received 30 November 1991
Revision accepted 4 November 1992